IEEE Access
Multidisciplinary | Rapid Review | Open Access Journal

Received 11 July 2022, accepted 24 July 2022, date of publication 1 August 2022, date of current version 8 August 2022.

*Digital Object Identifier 10.1109/ACCESS.2022.3195172*

RESEARCH ARTICLE

# Synergetic Control Strategy for Water Hammer Wave and Mass Wave in Hydropower Station With Downstream Channel

**TIANYU ZHANG, JIANZHONG ZHOU, YONGCHUAN ZHANG, YANG LIU, AND YUXIN LI**
School of Civil and Hydraulic Engineering, Huazhong University of Science and Technology, Wuhan 430074, China
Hubei Key Laboratory of Digital Valley Science and Technology, Wuhan 430074, China

Corresponding author: Jianzhong Zhou (jz.zhou@hust.edu.cn)

This work was supported by the Key Program of the National Natural Science Foundation of China under Grant U1865202.

**ABSTRACT** This paper investigates the synergetic control strategy for water hammer wave and mass wave in hydropower station with downstream channel. Firstly, the mathematical model of hydropower station with downstream channel (HSDC) and hydropower station with downstream channel and surge tank (HSDCST) are established. Then, the controller formula of HSDC and HSDCST are derived using the synergetic theory. Furthermore, it is parsed that the dynamic characteristics of HSDC and HSDCST to various disturbances under synergetic control strategy. Finally, the robustness and applicability of synergetic control strategy for HSDC and HSDCST are analyzed. The results indicate that the hydropower station under the synergetic control strategy has excellent dynamic characteristics with employing sensitive response, small overshoot, fast attenuation speed and no static error. The synergetic control strategy is superior to the PID control strategy under various disturbances in controlling the amplitude of water hammer wave in HSDC, which is down 12.5%. The attenuation of mass wave in HSDCST under synergetic control strategy is faster, and the settling time is 6.16s less than that of PID control strategy. Compared with PID control strategy, it is the robustness of synergetic control strategy that are much more advantageous for HSDC and HSDCST. Specifically, RI value is about 1.65, 0.18 for HSDC and 2.21, 0.25 for HSDCST under synergetic control strategy, while it is about 3.05, 1.20 and 3.32, 1.30 under PID control strategy. Moreover, the synergetic control strategy has a wide applicability in controlling the water hammer wave in HSDC and mass wave in HSDCST.

**INDEX TERMS** Hydropower station, downstream channel, synergetic control strategy, dynamic characteristics, robustness.

## I. INTRODUCTION

Many large hydropower stations have been built successively and most of them are on major rivers and basins in China [1]. Not only do they undertake the task of generating electricity, but also, not to be overlooked, have responsibility for irrigation [2]. Thus, their outlet is generally downstream channels, whose water level varies with the flow of hydropower station [3]. It is more practical to deal with the downstream boundary according to the relation of water level and flow.

The downstream channel is no longer regarded as an infinite reservoir that the water level of it is simplified as a constant but calculated according to the downstream flow [4]. It makes the research for the stability of hydropower stations more accurate but increases the difficulty for the derivation of formulas and the design of control strategies during the transient in hydropower station.

Modeling of hydropower station yields a nonlinear model, including the relationship of downstream level to flow, the head loss in pipeline, the characteristics of flow and torque, the electromagnetic system in generator, the hydraulic follow-up device and so on [5], [6]. Broadly used in hydropower station at present, PID control strategy is linear

The associate editor coordinating the review of this manuscript and approving it for publication was F. R. Islam.

mechanism [7], [8]. Therefore, it is difficult for nonlinear system to get better dynamic characteristics under PID control strategy.

Furthermore, as the hydropower station mainly takes on regulating task in the power grid, it often changes its operating state [9]. The hydropower station being in transient process may bring about many accidents [10]. The water hammer wave from pipeline system causes the variation of speed, running beyond the rated power and deviation from the optimal operating condition area, which will reduce the service of unit. The mass wave from surge tank contributes to the continuous low frequency oscillation in the hydropower station, which will destabilize the hydropower station or even expand into the power system. It is not only water hammer wave but also mass wave that must be suppressed during transient process in hydropower station. Therefore, it is necessary to find a better control strategy to improve the dynamic response quality of the hydropower station.

At present, there are many nonlinear control methods, such as control [11], [12], control [13], [14], control [15], [16], control [17], [18], control [19], [20], control [21]. Summarizing the research of the above references, there are few investigations on the good control effect on both water hammer wave in hydropower station with downstream channel (HSDC) and mass wave in hydropower station with downstream channel and surge tank (HSDCST). Hence, it is urgent to find a control strategy to fill this gap. As a nonlinear control theory, the synergetic control strategy performs excellent in multi-variable comprehensive control. In this paper, it is applied for the design of the controller to suppress the amplitude of water hammer wave and attenuation of mass wave.

For synergetic control strategy, it is the application of synergetic theory in the control field. The basic idea of synergetic control is to generate cooperative behaviors in the system through the synergetic controller and guide all parts of the system to reach the equilibrium point harmoniously. Under synergetic control strategy, manifold is a constraint condition defined in the system state space, which reflects the requirements for system control performance, and is also the attractor of the closed-loop system. The formation of attractor reflects the directional self-organization process. The self-organization behavior makes the system produce a new ordered structure, which has the importance that the original system does not have quality [22].

The synergetic control theory is initially successfully applied in the control of power electronic converters, mainly Buck circuit, Boost circuit and their multiple parallel control. Subsequently, it applied in motor control, aviation and other fields. At present, its application in power system mainly focuses on generator control, FACTS device, high-voltage direct current power transmission, wind turbine control, and has made rich achievements [23], [24].

Zhu *et al.* [25] proposed the integrated synergetic controller, which can enhance both the terminal voltage control and mechanical power tracking performances, embodying a more accurate precision and shorter settling time under different operating conditions. Zhou *et al.* [26] applied the synergetic control strategy to the hydraulic turbine governing system, and verified the superiority of dynamic characteristics and robustness through the numerical simulation experiment of load disturbance and three short circuit fault conditions. In order to control the frequency of small and medium-sized hydropower stations, Huang *et al.* [27] investigated a kind of a fixed-time synergetic controller to overcome the disadvantages of finite-time stability and verified its effectiveness and superiority through the comparison of several control strategies under different operation conditions. Zhao *et al.* [28] presented an improved synergetic excitation controller that it can enhance the stability of voltage and transient for the system by changing the adaptive strategy of the control parameters under various working conditions, which is proved on a single-machine infinite-bus power system. Zhao *et al.* [29] proposed a decentralized nonlinear power system stabilizer based on the synergetic control theory, which can provide sufficient damping to the power system in a large operating range and has good robustness by simulation. Ni *et al.* [30] designed a variable speed synergetic controller to solve the problem of chaotic oscillation in power systems. It can adjust the convergence speed to improve the regulation quality according to the dynamic response automatically. Bouchama *et al.* [31] developed an adaptive fuzzy power system stabilizer, which is insensitive to the change of system parameter. It has been proved that the stabilizer can suppress the oscillation in power system and has strong robustness through load disturbance experiments on single-machine infinite bus system and multi-machine power system. Ademoye *et al.* [32] designed a decentralized synergetic controller variable parameter for power system oscillation with PSO algorithm optimizing the gain, which has superior performance on two-area power system by simulation. Veselov *et al.* [33] applied the synergetic control theory to locomotive traction and proposed a new method for locomotive traction controller synthesis, which reduced the energy loss of electric traction drive unit.

This paper aims to study the synergetic control strategy for both water hammer wave in HSDC and mass wave in HSDCST. The contribution and novelty of paper are:

(1) Design the controller for HSDC and HSDCST based on synergetic theory.

(2) Illuminate the dynamic characteristics of HSDC and HSDCST under synergetic control strategy.

(3) Analyze the robustness of synergetic control strategy for HSDC and HSDCST.

(4) Account the applicability of synergetic control strategy in hydropower station.

The main chapters of this paper are arranged as follows. The mathematical model of HSDC and HSDCST are established, and the basic principle of synergetic control strategy is given in section II. The synergetic control strategy for HSDC and HSDCST are deduced in section III. The advantage of synergetic control strategy in controlling both HSDC and HSDCST is illustrated through the analysis of dynamic characteristics, compared with PID control strategy in section IV.

The robustness and applicability of synergetic control strategy for HSDC and HSDCST are studied in section V. The summary and conclusions are presented in section VI.

## II. MATHEMATICAL MODEL

In this section, the mathematical model of HSDC and HSDCST considering the relationship between downstream water level and flow are established at the very beginning. The structure diagram of hydropower station under synergetic control strategy is shown in Fig. 1. Then, the concept of synergetic theory is given, which lays a foundation for designing controller of HSDC and HSDCST.

### A. MATHEMATICAL MODEL

The mathematical model established in this paper should be able to accurately express the dynamic characteristics of hydropower stations with downstream channel. Therefore, on the basis of transient flow theory, turbine control and calculation of regulation guarantee theory, the following hypotheses are proposed in this paper.

(1) The walls of a pressurized pipeline and the water inside are rigid. Therefore, the rigid water hammer theory is used to calculate the water hammer pressure caused by the change of guide vane opening.

(2) The water level of the downstream channel is not constant but has a quadratic radical relationship with the flow of the hydropower station. It can be expressed as $H_d = K\sqrt{Q} + B$, where $H_d$ is the water level of downstream channel, $K$, $B$ is the coefficient of the relationship between the water level and flow, and $Q$ is the flow into the downstream channel.

(3) The flow characteristics and torque characteristics of turbine show a complex nonlinear relationship, which is difficult to be expressed analytically. In this paper, the control of hydropower station under small disturbance is studied, and the six-parameter model of turbine is adopted here.

(4) Since the existence of power grid can improve the stability of hydropower station, the regulation guarantee calculation of hydropower station is generally considered as the isolated condition. The first-order model of generator can satisfy the requirements of investigation.

(5) It is considered that the relay and follow-up hydraulic device have no dead zone and saturation link.

HSDC and HSDCST are described mathematically based on the above assumptions, of which the concise pictures are given in Fig. 2.

The hydroelectric unit equations of HSDC and HSDCST are the same, including turbine, generator and servo device, which can be presented as follows:

The characteristics equation of turbine [4], [34]:

$$q_t = e_{qh}h + e_{qx}x + e_{qy}y \tag{1}$$

$$m_t = e_h h + e_x x + e_y y \tag{2}$$

where $e_h$, $e_x$, $e_y e_{qh}$, $e_{qx}$, $e_{qy}$ is the transfer coefficients of turbine, and $q_t$ $m_t$, $h, x, y$ is the relative deviation value, which represent the turbine flow, the turbine torque. the water head, the speed, the guide vane.

The rotation equation of generator [35]:

$$T_a \frac{\mathrm{d}x_t}{\mathrm{d}t} = m_t - e_g x_t - m_g \tag{3}$$

where $T_a$ is the time constant of generator, $e_g$ is generator self-regulation coefficient.

The dynamic equation of servo device [11]:

$$\frac{\mathrm{d}y}{\mathrm{d}t} = \frac{1}{T_y}(u - y) \tag{4}$$

where $T_y$ is the servo device inertia time constant, $u$ is the output of controller.

However, there are great differences between HSDC and HSDCST in the model of hydraulic system. For HSDC, its penstock is directly connected with the downstream channel, so the unsteady flow in penstock can be described as follows [36]:

$$\frac{L_t}{gA_t}\frac{\mathrm{d}Q_t}{\mathrm{d}t} = H_u - H_d - H - h_t \tag{5}$$

The relative deviation value form of penstock:

$$T_{wt}\frac{\mathrm{d}q_t}{\mathrm{d}t} = -\frac{K\sqrt{Q_0}}{H_0}\left(\sqrt{q_t + 1} - 1\right) - h - \frac{2h_{t0}}{H_0}q_t \tag{6}$$

where $T_{wt}$ is flow inertia time constant of penstock, the expression of it is $T_{wt} = L_t Q_t / (gA_t H_0)$. $h_{t0}$ is the initial value of head loss in penstock. $Q_0$, $H_0$, is the initial value of flow and water head in turbine.

For HSDCST, the downstream surge tank is installed in the hydropower station. The end of the penstock is a surge tank, which is connected with the downstream channel through the tailwater tunnel. Correspondingly, the dynamic equation of the penstock is rewritten as follows:

$$T_{wt}\frac{\mathrm{d}q_t}{\mathrm{d}t} = -z - h - \frac{2h_{t0}}{H_0}q_t \tag{7}$$

where $z$ is the relative value of the water level in surge tank.

The momentum equation in the tailwater tunnel is as follows [37]:

$$\frac{L_y}{gA_y}\frac{\mathrm{d}Q_y}{\mathrm{d}t} = Z - H_d - h_y \tag{8}$$

where $L_y$ is the length, $A_y$ is the area, and $h_y$ is the head loss of penstock.

The relative deviation value form of tailwater tunnel:

$$T_{wy}\frac{\mathrm{d}q_y}{\mathrm{d}t} = z - \frac{K\sqrt{Q_0}}{H_0}\left(\sqrt{q_y + 1} - 1\right) - \frac{2h_{y0}}{H_0}q_y \tag{9}$$

where $T_{wy}$ is flow inertia time constant of tailwater tunnel, the expression of it is $T_{wy} = L_y Q_y / (gA_y H_0)$. $q_y$ is the relative value of flow in tailwater tunnel.

The continuous equation of surge tank [38]:

$$\frac{\mathrm{d}z}{\mathrm{d}t} = \frac{1}{T_F}(q_t - q_y) \tag{10}$$

where $T_F$ is the flow inertia time constant of surge tank.

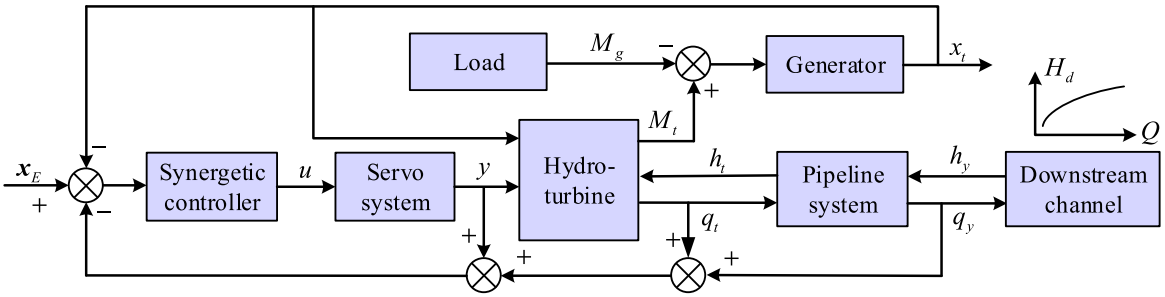


**FIGURE 1.** Structure diagram of hydropower station under synergetic control strategy.

By integrating (1)-(6), the state equation of HSDC can be obtained, as shown in following equation. (11), as shown at the bottom of the page.

For HSDCST, its state equation can be derived to following equation, by combining (1)-(4) and (7)-(10). (12), as shown at the bottom of the page.

The measured data of the hydropower station are selected to verify the accuracy of model. It should be noted here that due to the limited measured data of the hydropower stations [39], the example is a hydropower station with upstream surge chamber. The main research purpose of this paper is to design the controller of HSDC and HSDCST, so (11) and (12) are modified under this theoretical system, and finally simulated verification is conducted. The comparison results are shown in the Fig. 3.

For the comparison between simulation and measured data, they showed a remarkable degree of consistency. Specifically speaking, the maximum error of y is 1.65%, and the average error is 2.55%. As accuracy. As can be seen from the above, the model for output, its maximum is 2.55%, and the average error of the whole process is 0.35% with high has been verified to some extent, and the analysis of stability and controller design based on it has high reliability.

### B. BASIC PRINCIPLE OF SYNERGETIC CONTROL STRATEGY

Synergetic control theory is a state-space method based on modern mathematics and synergetic theory. It provides an effective means for the design of feedback controller of nonlinear system by utilizing the nonlinear characteristics of the system itself. The nonlinear control system using synergetic control has global stability running on manifold, and it is easy to implement in engineering. The basic principle and design process of synergetic control strategy are presented as follows.

For a $n$-dimensional nonlinear affine system that can be expressed as following (13), there are macro variables

$$\begin{cases} \dot{y} = \dfrac{1}{T_y}(u - y) \\ \dot{q}_t = \dfrac{1}{T_{wt}}\left[\dfrac{K\sqrt{Q_0}}{H_0}\left(1 - \sqrt{q_t + 1}\right) - \left(\dfrac{2h_{t0}}{H_0} + \dfrac{1}{e_{qh}}\right)q_t + \dfrac{e_{qx}}{e_{qh}}x_t + \dfrac{e_{qy}}{e_{qh}}y\right] \\ \dot{x}_t = \dfrac{1}{T_a}\left[\dfrac{e_h}{e_{qh}}q_t + \left(e_x - e_g - \dfrac{e_h e_{qx}}{e_{qh}}\right)x_t + \left(e_y - \dfrac{e_h e_{qy}}{e_{qh}}\right)y - m_g\right] \end{cases} \tag{11}$$

$$\begin{cases} \dot{y} = \dfrac{1}{T_y}(u - y) \\ \dot{q}_t = \dfrac{1}{T_{wt}}\left[-z - \left(\dfrac{1}{eqh} + \dfrac{2h_{t0}}{H_0}\right)q_t - \dfrac{e_{qx}}{e_{qh}}x_t - \dfrac{e_{qy}}{e_{qh}}y\right] \\ \dot{z} = \dfrac{1}{T_F}(q_t - q_y) \\ \dot{q}_y = \dfrac{1}{T_{wy}}\left[z - \dfrac{K\sqrt{Q_0}}{H_0}\left(\sqrt{q_y + 1} - 1\right) - \dfrac{2h_{y0}}{H_0}\right] \\ \dot{x}_t = \dfrac{1}{T_a}\left[\dfrac{e_h}{e_{qh}}q_t + \left(e_x - e_g - \dfrac{e_h e_{qx}}{e_{qh}}\right)x_t + \left(e_y - \dfrac{e_h e_{qy}}{e_{qh}}\right)y - m_g\right] \end{cases} \tag{12}$$

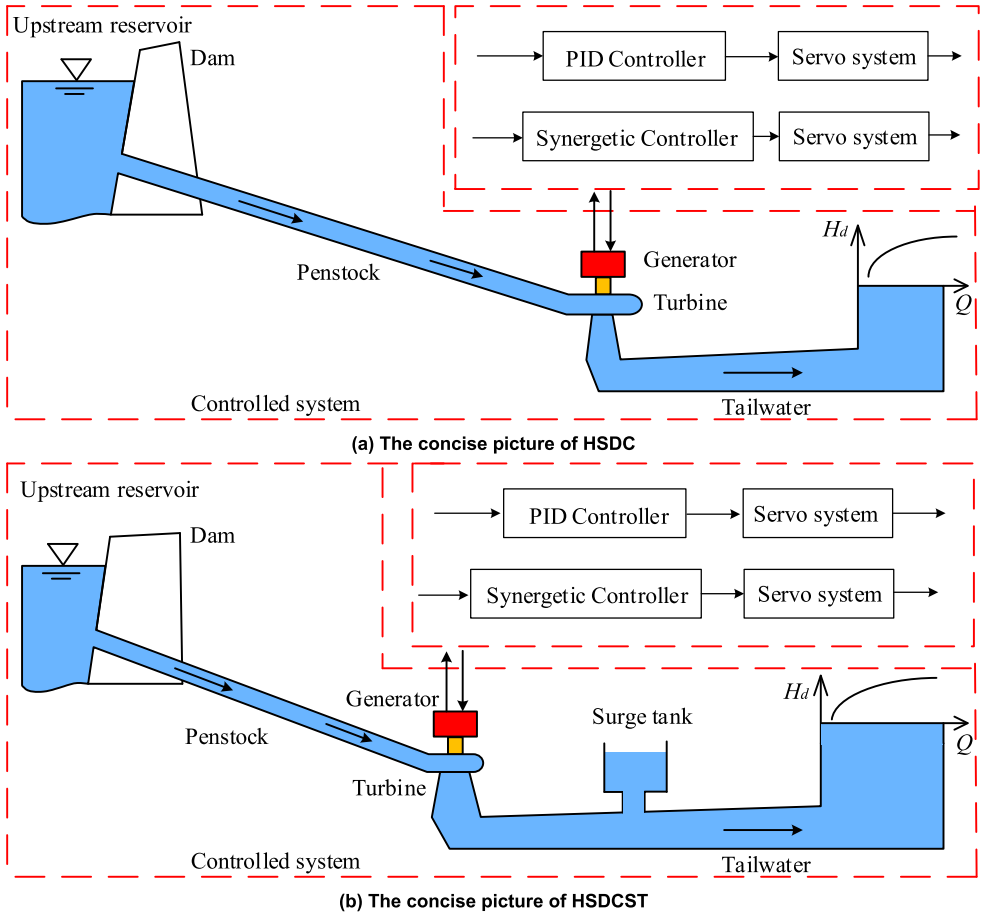


**FIGURE 2.** Structure diagram of hydropower station under synergetic control strategy.

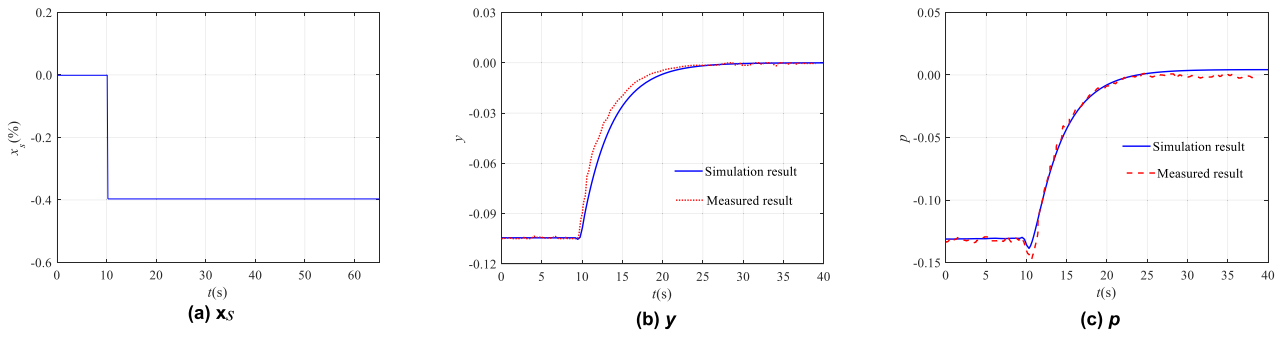


**FIGURE 3.** Comparisons of simulation results and measured results.

$\psi(x,t)$

$$\begin{cases} \dot{x} = f(\boldsymbol{X},t) + g(\boldsymbol{X})\boldsymbol{u} \\ y = h(\boldsymbol{X}) \end{cases} \tag{13}$$

that makes the following equation true [27].

$$T\dot{\psi} + \psi = 0\,(T > 0) \tag{14}$$

Define $\psi(x,u) = 0$ as a manifold. If the stability of the system under the controller can be guaranteed, the system must converge to the equilibrium point along the manifold after perturbation. Because the macro variable is a function of the state variable, and the state variable is a function of time. So, the (14) can be written (15).

$$T\frac{\mathrm{d}\psi}{\mathrm{d}x}f(\boldsymbol{X},\boldsymbol{u},t) + \psi = 0\,(T > 0) \tag{15}$$

From (15) we can deduce the control equation.

$$\boldsymbol{u} = F(\boldsymbol{X},\psi(\boldsymbol{X},t),T) \tag{16}$$

The system under the action of synergetic control strategy, has better global stability, better robustness to system parameters, and can suppress noise.

## III. DESIGN OF SYNERGETIC CONTROL STRATEGY

Synergetic control strategy is a kind of nonlinear system control method. The design of synergetic control strategy mainly consists of two steps. The first step is the exact linearization of a nonlinear system. The second step is to choose the appropriate macro variable so that the system converges quickly to the manifold. In this section, the HSDC and HSDCST under synergetic control strategy are designed according to its basic principle in Section II.B.

### A. EXACT LINEARIZATION

The purpose of control strategy design is to make the system reach a new equilibrium point under external disturbance quickly and smoothly. $\dot{\boldsymbol{x}} = 0$ is true at the new equilibrium $\boldsymbol{x}_E$ [40]. Therefore, the new equilibrium point of HSDC is shown in (17), and the new equilibrium point of HSDCST under load disturbance is given in (18), where the subscript E represents the value of each variable at equilibrium point. The expansion of them are presented in Appendix A.

$$\boldsymbol{x}_{E1} = (y_{E1}, q_{tE1}, x_{tE1}) \tag{17}$$

$$\boldsymbol{x}_{E2} = \left(q_{yE2}, y_{E2}, x_{tE2}, z_{E2}, q_{tE2}\right) \tag{18}$$

Since it is easier to design controllers and judge the stability of closed-loop systems for linear systems using synergetic theory [36], feedback linearization can be performed on the state equation of HSDC. Having selected the output function $h_1(\boldsymbol{X}) = x_t$, the relative order of HSDC is three. Therefore, (7) is rewritten as (19).

$$\begin{cases} Z_1 = h_1(\boldsymbol{X}) = x_t \\ \dot{Z}_1 = Z_2 = L_{f1}h_1(\boldsymbol{X}) = \dot{x}_t \\ \dot{Z}_2 = Z_3 = L_{f1}^2 h_1(\boldsymbol{X}) = -\dfrac{\eta_1 y}{T_y} + \eta_2\dot{q}_t + \eta_3\dot{x}_t \\ \dot{Z}_3 = L_{f1}^3 h(\boldsymbol{X}) + \left[L_{g1}L_{f1}^2 h_1(\boldsymbol{X})\right]u \\ = -\dfrac{\xi_1}{T_y}y + \left(\xi_2 - \dfrac{\xi_3}{\sqrt{1+q_t}}\right)\dot{q}_t + \xi_4\dot{x}_t + \dfrac{\xi_1}{T_y}u \end{cases} \tag{19}$$

where, $\boldsymbol{Z} = (Z_1, Z_2, Z_3)$ is the state variables of the system of HSDC after feedback linearization.

Similarly, the relative order of HSDCST is five with $h_2(\boldsymbol{X}) = x_t$ as the output function. By coordinate transformation, (12) is converted into the form of following equation.

$$\begin{cases} W_1 = h_2(\boldsymbol{X}) = x_t \\ \dot{W}_1 = W_2 = L_{f2}h_2(\boldsymbol{X}) = \dot{x}_t \\ \dot{W}_2 = W_3 = L_{f2}^2 h_2(\boldsymbol{X}) = -\dfrac{a_1 y}{T_y} + a_2\dot{q}_t + a_3\dot{x}_t \\ \vdots \\ \dot{W}_3 = W_4 = L_{f2}^3 h_2(\boldsymbol{X}) = -\dfrac{b_1 y}{T_y} + b_2\dot{q}_t + b_3\dot{z} + b_4\dot{x}_t \\ \dot{W}_4 = W_5 = L_{f2}^4 h_2(\boldsymbol{X}) = -\dfrac{c_1 y}{T_y} + c_2\dot{q}_t \\ \quad + c_3\dot{z} + c_4\dot{q}_y + c_5\dot{x}_t \\ \dot{W}_5 = L_{f2}^5 h_2(\boldsymbol{X}) + \left[L_{g2}L_{f2}^4 h_2(\boldsymbol{X})\right]u \\ = -\dfrac{d_1}{T_y}y + d_2\dot{q}_t + d_3\dot{z} + \left(d_4 - \dfrac{d_5}{\sqrt{1+q_y}}\right)\dot{q}_y \\ \quad + d_6\dot{x}_t + \dfrac{d_1}{T_y}u \end{cases} \tag{20}$$

Where, $W = (W_1, W_2, W_3, W_4, W_5)$ is the state variables of the system of HSDCST after feedback linearization.

### B. DESIGN OF CONTROL STRATEGY

The unit speed is the most important control objective of the hydropower station under small load disturbance. $Z_1$ can fully represent the unit speed, which is taken as a component of the macro variable. Secondly, $Z_2$ will be ignored in the macro variable since it is a part of $Z_3$. Therefore, the macro variable is determined to be following equation.

$$\psi = k_1(Z_1 - Z_{1E}) + k_2(Z_3 - Z_{3E}) \tag{21}$$

where $Z_{1E}$, $Z_{3E}$ is the equilibrium point of the linear system after coordinate transformation, and $k_1$, $k_2$ is controller parameter of synergetic control strategy for HSDC, which can be obtained by substituting (17) into (19).

Substituting (21) into dynamic (15) of macro variable attenuation, the following equation can be obtained.

$$k_1(Z_1 - Z_{1E}) + k_1 T Z_2 + k_2(Z_3 - Z_{3E}) + k_2 T\dot{Z}_3 = 0 \tag{22}$$

Finally, the control strategy of guide vane can be obtained by substituting (19) into (22), as shown in the following equation.

$$u = \frac{T_y}{\xi_1}\left[-\frac{k_1}{Tk_2}x_t + \left(\frac{\eta_1}{TT_y} + \frac{\xi_1}{T_y}\right)y - \left(\frac{\eta_3}{T} + \xi_4 + \frac{k_1}{k_2}\right)\dot{x}_t + \left(-\xi_2 - \frac{\eta_2}{T} + \xi_3\frac{1}{\sqrt{1+q_t}}\right)\dot{q}_t - \frac{\eta_1 y_E}{TT_y}\right] \tag{23}$$

For HSDCST, the dynamic response of $x_t$ is mainly composed of two parts, one is called head wave caused by pipeline, belonging to water hammer wave, which is high frequency; the other is called wake wave caused by surge tank, belonging to mass wave, which is low frequency. Both of them must be well controlled at the same time so that the HSDCST can have excellent dynamic performance. Therefore, $W_1$ representing the speed will be an important part of the macro variable. Since $W_5$ can be linearly represented by $W_2$, $W_3$, and $W_4$, only $W_5$ is selected as a component of the macro variable. As thus, the macro variable consists of $W_1$ and $W_5$, which is written in this form as follows:

$$\psi = \lambda_1(W_1 - W_{1E}) + \lambda_2(W_5 - W_{5E}) \tag{24}$$

where $W_{1E}$, $W_{5E}$ are computed from the simultaneous (18) and (20), and $\lambda_1$, $\lambda_2$ is controller parameter of synergetic control strategy for HSDCST.

Similarly, having combined (15), (20) and (24), the expression of the control quantity can be yield, as shown in the following equation.

$$u = \frac{T_y}{d_1}\left[-\frac{\lambda_1}{T\lambda_2}x_t + \left(\frac{c_1}{TT_y} + \frac{d_1}{T_y}\right)y - \left(\frac{\lambda_1}{\lambda_2} + \frac{c_5}{T} + d_6\right)\dot{x}_t - \left(\frac{c_2}{T} + d_2\right)\dot{q}_t - \left(\frac{c_3}{T} + d_3\right)\dot{z} - \left(d_4 + \frac{c_4}{T} - d_5\frac{1}{\sqrt{1+q_y}}\right)\dot{q}_y - \frac{d_1}{TT_y}y_E\right] \tag{25}$$

## IV. DYNAMIC CHARACTERISTICS UNDER SYNERGETIC CONTROL STRATEGY

In this section, it is under synergetic control strategy that the dynamic characteristics of HSDC and HSDCST are investigated in extenso. First of all, the engineering examples of HSDC and HSDCST is taken, and the state equation under PID control strategy is given. Secondly, it is obtained that the dynamic response of HSDC and HSDCST under synergetic and PID control strategy. The dynamic characteristics of HSDC and HSDCST under synergetic control strategy is evaluated by quantitative indexes. Finally, the analysis of dynamic performances of synergetic control strategy for various disturbances is carried out.

### A. EXAMPLE OF DYNAMIC RESPONSES

In order to investigate the dynamic characteristics of hydropower station under synergetic control strategy, the real hydropower stations are taken as examples in this study. The basic parameters of HSDC is as follows: $H_0 = 120$ m, $Q_0 = 665$ m$^3$/s, $T_{wt} = 2.83$ s, $h_{t0} = 0.53$ m, $K = 0.004$, $e_h = 1.5$, $e_x = -1$, $e_y = 1$, $e_{qh} = 0.5$, $e_{qx} = 0$, $e_{qy} = 1$, $e_g = 0$, $T_a = 10.32$ s, $T_y = 0.2$ s, $m_g = -0.1$, $k_1 = 1.0$, $k_2 = 3.5$, $T_1 = 0.5$. The basic parameters of HSDCST is given: $H_0 = 80$ m, $Q_0 = 506$ m$^3$/s, $T_{wt} = 3.43$ s, $h_{t0} = 1.46$ m, $K = 0.004$, $e_h = 1.5$, $e_x = -1$, $e_y = 1$, $e_{qh} = 0.5$, $e_{qx} = 0$, $e_{qy} = 1$, $e_g = 0$, $T_a = 9.52$ s, $T_y = 0.2$ s, $m_g = -0.1$, $\lambda_1 = 1.0$, $\lambda_2 = 3.5$, $T_1 = 0.5$.

PID control strategy being a reference, the superiority of synergetic control strategy is illustrated. The formula of the former is given in the following equation [41].

$$u = -K_p x_t - K_i \int x_t - K_d \frac{dx_t}{dt} \tag{26}$$

where the $K_p$, $K_i$, $K_{d1}$ is the basic data of PID control strategy, its value is usually determined by Stein formula [42], i.e. $K_{p1} = 7T_a/9T_{wt}$, $K_{i1} = T_a/4.5T_{wt}^2$, $K_{d1} = T_a/3$, when applied to the control of guide vane in hydropower station. For the engineering example given above, the calculation result of HSDC is $K_{p1} = 2.8363$, $K_{i1} = 0.2863$ s$^{-1}$, $K_{d1} = 3.44$ s, and that of HSDCST is $K_{p2} = 2.1462$, $K_{i1} = 0.1777$ s$^{-1}$, $K_{d1} = 3.1733$ s.

Equation (26) is substituted into (11) to obtain the state equation of HSDC under PID control strategy, which is given in Appendix A. Likewise, the state equation of HSDCST under PID control strategy can be yield by combing (12) and (26), which is also given in Appendix A.

By adding (23) to (11), the state equation of HSDC under synergetic control strategy can be obtained. The dynamic response of HSDC under synergetic control strategy is given in Fig. 2. Substitute (25) into (12) will yield the state equation of HSDCST under synergetic control strategy, whose dynamic response is shown in Fig. 2. Being a reference, the dynamic responses of HSDC and HSDCST under PID control strategy are also given in Fig. 2. Meanwhile, the integral square time square error (ISTSE) [43] of dynamic response is provided in Fig. 2. It amplifies the weight of time and error in the evaluation of system performance, not only ensures the fastest rise time and the shortest settling time, but also greatly reduces the system overshoot, which equation is shown as follows:

$$\text{ISTSE} = \int_0^\infty t^2 e^2(t)dt \tag{27}$$

where $t$ is simulation time, $e(t)$ is dynamic response of state variables.

### B. ANALYSIS OF DYNAMIC CHARACTERISTICS

In order to evaluate the two control strategies quantitatively, it is calculated that the indicator of dynamic response of HSDC and HSDCST under synergetic and PID control strategy, such as amplitude, peak time, rise time, settling time and overshoot according to the results of characteristics in Fig. 4, which is given in Table 1 and Table 2.

Specially, for settling time, it refers to the time when the speed enters 0.4% bandwidth and is no longer exceeded according to the regulation guarantee calculation specification [44]. The definition of 0.4% bandwidth is given, as shown in the following equation.

$$\exists t_s,\ when\ t_i > t_s,\ \ s.t.\ \left|\frac{n(t_i) - n_0}{n_0}\right| \le 0.4\% \quad (i = 1, 2, \ldots) \tag{28}$$

where $t_i$ is the simulation time, $t_s$ is the settling time, $n(t_i)$ is the unit speed, and $n_0$ is the steady speed. For the dynamic response of HSDC:

(1) As shown in Fig. 4 (b)(c), for the overall characteristic process of $x_t$ and $y$, the effect of synergetic control strategy is significantly better than that of PID control strategy. In terms of the composite indicator ISTSE, the value of it under the former is obviously smaller than under of the latter. The ISTSE of $x_t$ is 8.8253e-06 and the ISTSE of $y$ is 3.8026e-06 under synergetic control while the former is 1.1676e-05 and the latter is 3.8026e-06 under PID control strategy. It is the same phenomenon that is illustrated forcefully by quantitative index in Table 1.

(2) Specifically, the maximum amplitude of $x_t$ is 0.035 under synergetic control strategy and 0.040 under PID

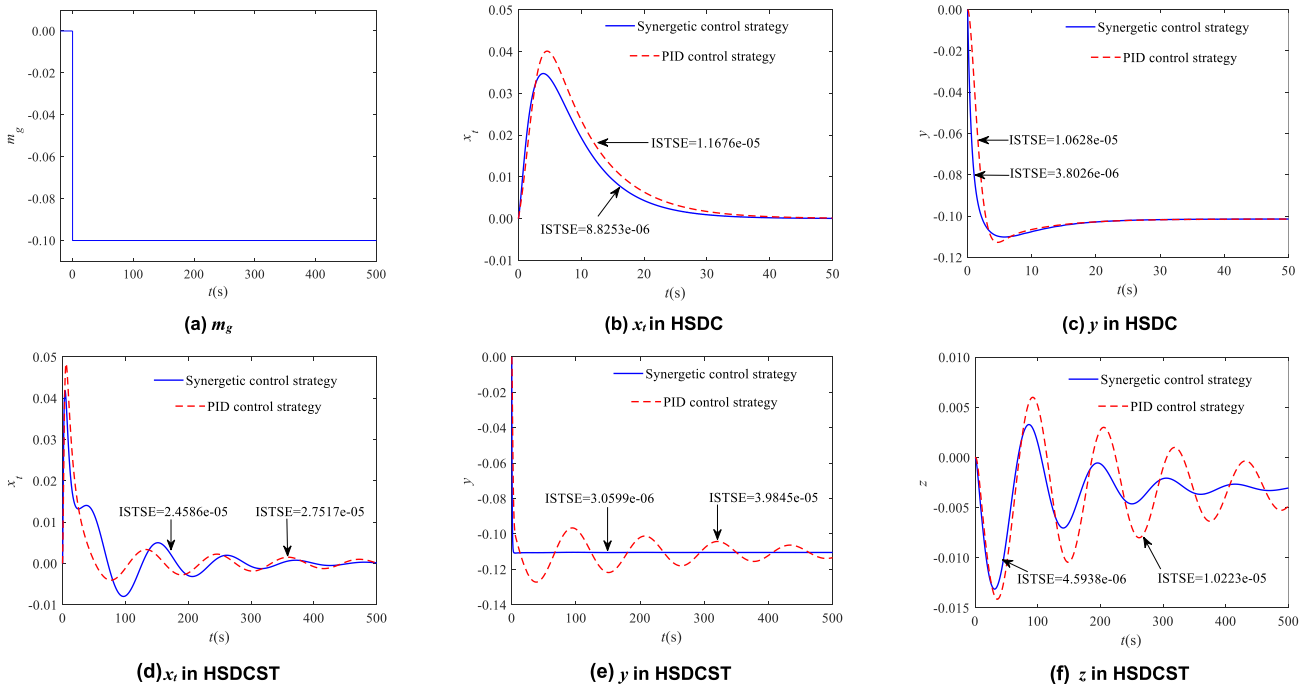


(a) $m_g$ (b) $x_t$ in HSDC (c) $y$ in HSDC

(d) $x_t$ in HSDCST (e) $y$ in HSDCST (f) $z$ in HSDCST

**FIGURE 4.** The dynamic responses in HSDC and HSDCST under synergetic and PID control strategy.

**TABLE 1.** Indexes of regulation quality for HSDC under synergetic and PID control strategy.

| Control strategy | Amplitude | | Peak time (s) | | Settling time (s) | Rise time (s) | Overshoot |
|---|---|---|---|---|---|---|---|
| | $x_t$ | $y$ | $x_t$ | $y$ | $x_t$ | $y$ | $y$ |
| Synergetic | 0.035 | -0.110 | 3.930 | 5.094 | -- | 2.294 | 1.476 |
| PID | 0.040 | -0.113 | 4.626 | 4.821 | 4.819 | 2.878 | 4.244 |

**TABLE 2.** Indexes for response quality of HSDCST under synergetic and PID control strategy.

| Control strategy | Amplitude | | | Peak time (s) | | | Rise time (s) | | Overshoot | | Settling time (s) |
|---|---|---|---|---|---|---|---|---|---|---|---|
| | $x_t$ | $y$ | $z$ | $x_t$ | $y$ | $z$ | $y$ | $z$ | $y$ | $z$ | $x_t$ |
| Synergetic | 0.042 | -0.111 | -0.013 | 3.878 | 4.159 | 31.310 | 2.480 | 6.312 | 0.006 | 3.194 | 5.286 |
| PID | 0.048 | -0.127 | -0.014 | 5.579 | 38.178 | 35.457 | 12.680 | 8.074 | 0.152 | 3.516 | 9.630 |

control strategy, which decreases by 14.29%. Meanwhile, the $x_t$ reaches the peak value faster under the synergetic control strategy, about 0.7s earlier. This shows that the synergetic control strategy is superior in terms of rapidity compared with PID control strategy. The unit enters 0.4% bandwidth faster under the PID control strategy is 4.819s, while it is always in bandwidth under the synergetic control strategy, which has better stability. It is good stability that the synergetic control produces. Moreover, there is no steady-state error in the characteristics of $x_t$ under synergetic control, which indicates that the control strategy meets the requirement of accuracy.

(3) For the characteristic index of guide vane opening, compared with PID control strategy, the amplitude and overshoot are smaller under synergetic control strategy and have better stability. Meanwhile, the peak time is slightly longer while the rise time is shorter. Not only does it not affect the overall rapidity, but also makes the dynamic response process of guide vane smoother, which is more conducive to the operation of servo device. Moreover, it meets the requirement of guide vane control accuracy with no static error.

For the dynamic response of HSDCST:

(1) It can be seen in Fig. 4 that HSDCST has an excellent dynamic response with rapid response, good convergence and no static error under the synergetic control strategy in terms of the dynamic response of $x_t$, $y$ and $z$, compared with PID control strategy.

(2) For dynamic response of $x_t$, the overall index ISTSE is 2.4586e-05 under the synergetic control strategy and 2.7517e-05 under the PID control strategy. Detailly, it reaches the peak value of 0.042 at 3.878s under the former the amplitude is 0.048 and the peak time is 5.579s under the latter. The amplitude of speed decreased by 14.29% and the response rate increased by 43.86%. Furthermore, the speed converges quickly under synergetic control, and the time to enter 0.4% bandwidth is 5.286s, while it takes 9.63s under PID control strategy.

(3) In terms of guide vane opening, the rapidity, stability and accuracy of dynamic response under synergetic control strategy are more superior, which are proved from ISTSE. It is 3.0599e-06 under synergetic control strategy while 3.9845e-05 under PID control strategy. In detail, the fluctuation

amplitude of guide vane opening is relatively small 14.41%. Meanwhile, the overshoot is only 0.006, which means that there is almost no overshoot. The response rate being fast, the peak time is 4.159s, and the rise time is 2.48s. However, they are 38.178 and 12.68 under PID control strategy respectively. In addition, its steady-state value is −0.1104 without static error.

(4) The synergetic control strategy also shows good performance to the fluctuation of the water level in the surge tank, under which the value of ISTSE is 4.5938e-06 while it is 1.0223e-05 under PID control strategy. The amplitude and overshoot are about 7.69% better than those under PID control strategy. For that under synergetic control, the rise time is 13.34% faster and the peak time is 27.92% faster. Obviously, the convergence of water level fluctuation of the surge tank is much faster under the synergetic control strategy.

For all above, the synergetic control strategy can not only greatly reduce the amplitude of high-frequency fluctuation corresponding to water hammer wave, but also accelerate the attenuation of low-frequency fluctuation corresponding to mass wave. At the same time, it has excellent dynamic characteristics in rapidity, stability and accuracy.

### C. ANALYSIS OF DYNAMIC PERFORMANCES TO VARIOUS DISTURBANCES

Due to the special working condition and environment in the electric system, the automation equipment will be interfered by external electromagnetic waves in the process of operation. In the harmonic disturbance of electric system, for the general disturbance, saw wave can be applied for excitation, because saw wave is composed of sine waves with different amplitude and finite times of different frequencies according to Fourier Analysis, that is, the basic waveform is sine wave. When the electric system is seriously disturbed, it can be excited by square wave, because the square wave is theoretically composed of more times with different frequencies and different amplitudes according to the Fourier transform, which is a way to investigate the stability of the system [45].

Therefore, the performance of the controller will be tested using sine wave, saw wave and square wave as excitation respectively in this section, of which the amplitude is −0.1 and the period is 100s, and the disturbances will last for two period. They are square disturbance, sine disturbance, and saw disturbance respectively, of which the dynamic process is shown in Fig. 5(a)-Fig. 7(a). Then the dynamic response of HSDC and HSDCST under various disturbances are given, as shown in Fig. 5(b)(e)(f)-Fig. 7(b)(e)(f). On this basis, standard deviation ($\sigma$) [46] is adopted to evaluate the output uncertainty of the hydropower station subjected to external random disturbance, as shown in the following equation. Meanwhile, the ISTSE are adopted to evaluate the performance of control strategy, as shown in Fig. 5(c)(g)-Fig. 7(c)(g).

$$\Delta_i = \sqrt{\sum_{t=0}^{Tsim} \left[O_i^{SCS}(t) - O_i^{PID}(t)\right]} \tag{29}$$

where $O_i^{SCS}(t)$ is the time-domain waveform of disturbed system state variables under synergetic control strategy, $O_i^{PID}(t)$ is the time-domain waveform of disturbed system state variables under PID control, $T_{\text{sim}}$ is the simulation time.

It can be seen from the above dynamic response results of hydropower station under various disturbances that the synergetic control strategy has a good effect in the control of water hammer wave and mass wave.

Specifically, in HSDC where only water shock wave exists, the response speed of $x_t$ in each peak region is faster and the overshoot is smaller under synergetic control strategy in Fig. 5(b)-Fig. 7(b). For HSDCST with mass wave, the synergetic control strategy shows good performance in the convergence of $x_t$ and $z$. As shown in Fig. 5(e)(f)- Fig. 7(d)(e), regardless of the type of disturbance, the dynamic response of $x_t$ and $z$ under synergetic control have completely damped after 500s in two periods while it needs twice as much time under PID control strategy. Meanwhile, the dynamic responses of HSDC and HSDCST can reach the equilibrium point accurately without steady-state error.

Meanwhile, the $\sigma$ and ISTSE of dynamic responses under synergetic control strategy are far less than these under PID control strategy from Fig. 5(c)(g)- Fig. 7(c)(f). As the $\sigma$ and ISTSE amplify the weight of time and error in evaluating the performance of system, it indicates that the synergetic control strategy can greatly reduce the overshoot of system while ensuring the fastest rising time and the shortest settling time. The above shows that the hydropower station adopts the synergetic control strategy under various disturbances, which can ensure its excellent stability and dynamic performances, and also prolong the service life of the governor and servo device.

### D. ANALYSIS OF DYNAMIC PERFORMANCES TO LOAD VARIATION

In an actual hydropower station, the load adjustments, such as load growth and load reduction, of the units are controlled by the guide vanes, which is difficult. The load adjustment processes usually take a long time. In order to implement performance measures on the basis of deviations from ideal waveforms, the load variation tracking is carried out in this section. Taking 10% load variation as an example, linear variation and ladder variation are adopted respectively [47]. The calculation results are shown in Fig. 8 and Fig. 9. The error, $\sigma$ and ITESE values of load tracking process are given in Table 3.

From the Fig. 8 and Fig. 9, the two control strategies can be roughly consistent throughout the process. However, it is clear that the synergistic strategy has a better control effect whether in local load variation or overall tracking. Under synergetic control strategy, the dynamic response of load has faster response speed, smaller overshoot, and smaller process errors.

For the quantitative indicators of tracking effectiveness, as presented in Table 3, compared with PID control strategy, the synergetic control strategy is more excellent. Specifically,

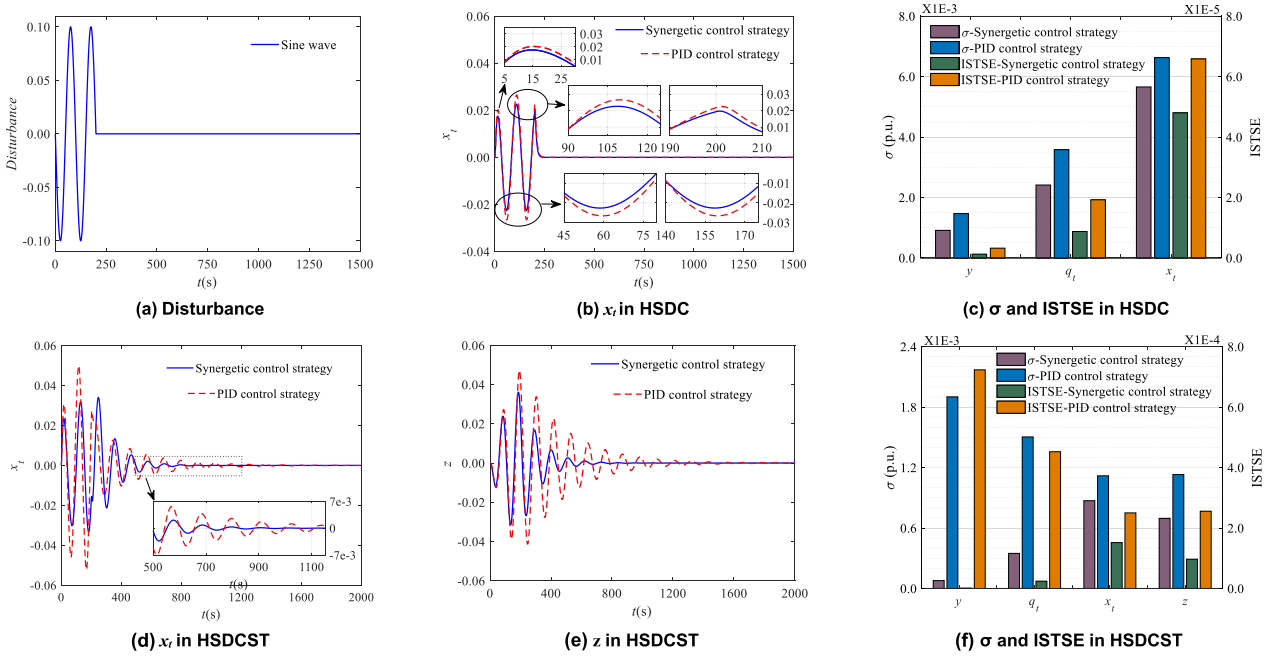


(a) Disturbance (b) $x_t$ in HSDC (c) σ and ISTSE in HSDC

(d) $x_t$ in HSDCST (e) z in HSDCST (f) σ and ISTSE in HSDCST

**FIGURE 5.** The dynamic responses and indexes for sine disturbance under synergetic and PID control strategy.

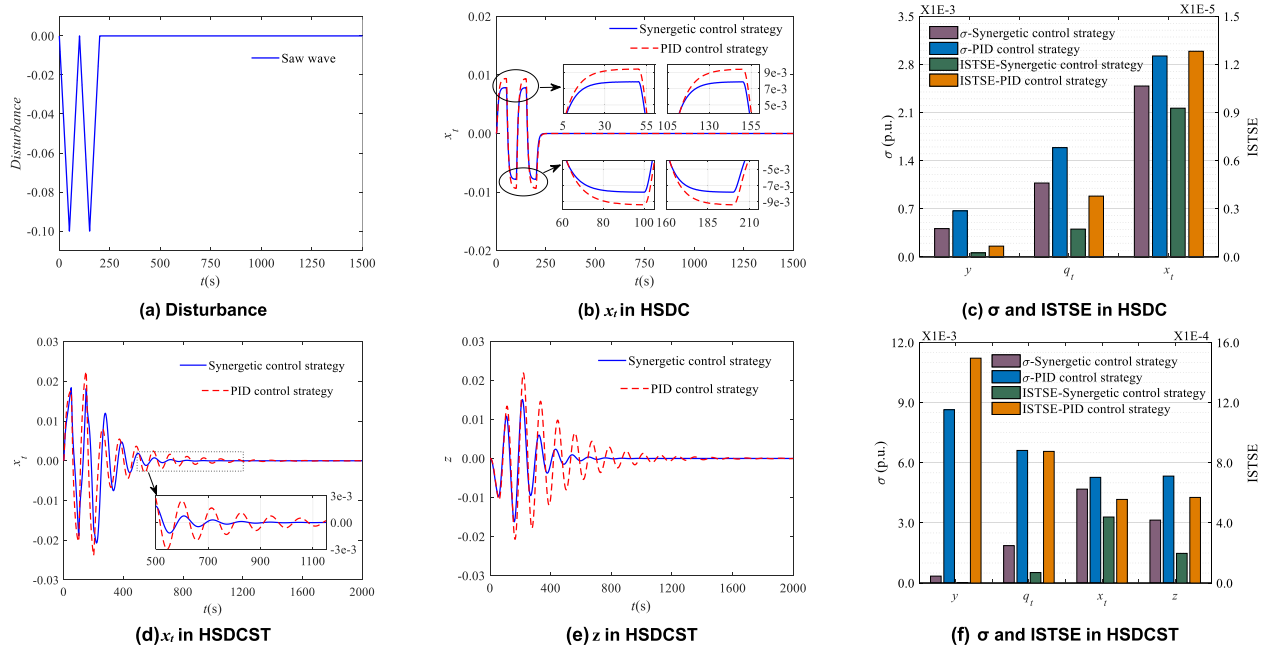


(a) Disturbance (b) $x_t$ in HSDC (c) σ and ISTSE in HSDC

(d) $x_t$ in HSDCST (e) z in HSDCST (f) σ and ISTSE in HSDCST

**FIGURE 6.** The dynamic responses and indexes for saw disturbance under synergetic and PID control strategy.

**TABLE 3.** Error indicators for ideal waveforms of load variation under synergetic and PID control strategy.

| Error indicators | $\lvert e\rvert_{\max}$ | | σ | | ISTSE | |
|---|---|---|---|---|---|---|
| | SCS | PID | SCS | PID | SCS | PID |
| Load line growth | 0.0036 | 0.0041 | 6.130e-04 | 7.0592e-04 | 1.8788e-07 | 2.4916e-07 |
| Load ladder growth | 0.0036 | 0.0041 | 8.670e-04 | 9.9570e-04 | 3.7585e-07 | 4.9575e-07 |
| Load line reduction | 0.0036 | 0.0041 | 6.130e-04 | 7.0513e-04 | 2.4860e-07 | 1.8789e-07 |
| Load ladder reduction | 0.0036 | 0.0041 | 8.672e-04 | 9.9578e-04 | 3.7602e-07 | 4.9579e-07 |

the error is around 0.0036 under synergetic control strategy, and it is about 0.0041 under PID. The load tracking error of hydropower station under synergetic control strategy is smaller. At the same time, the $\sigma$ and ISTSE are smaller under the synergetic control strategy, which can reflect the control process performance.

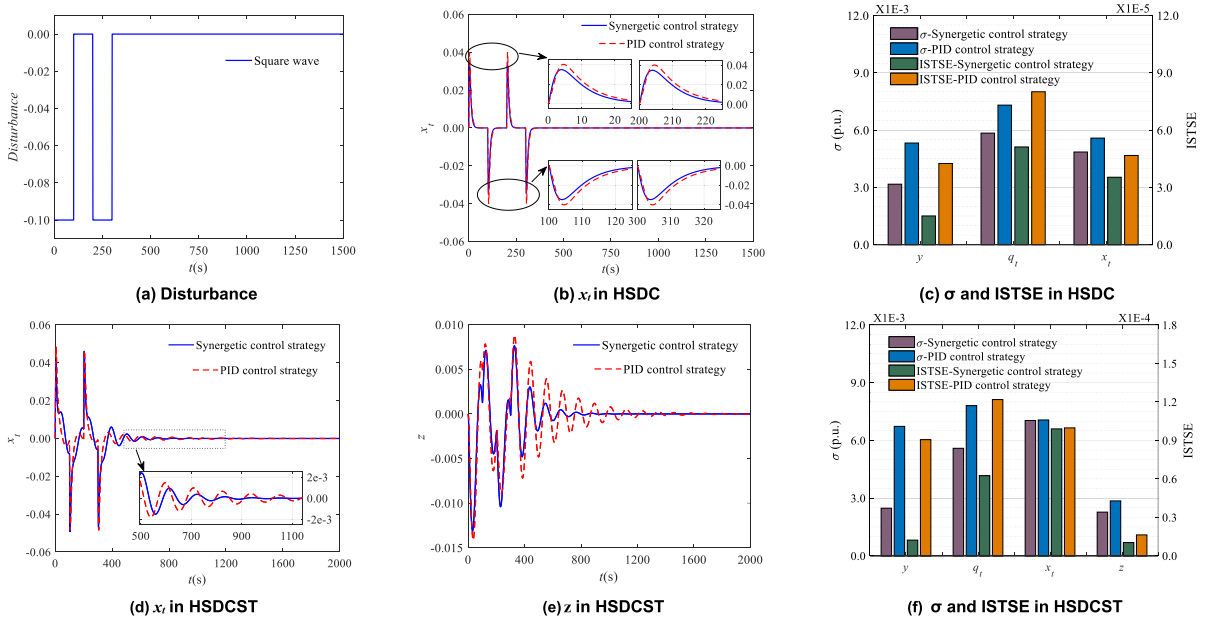


**FIGURE 7.** The dynamic responses and indexes for square disturbance under synergetic and PID control strategy.

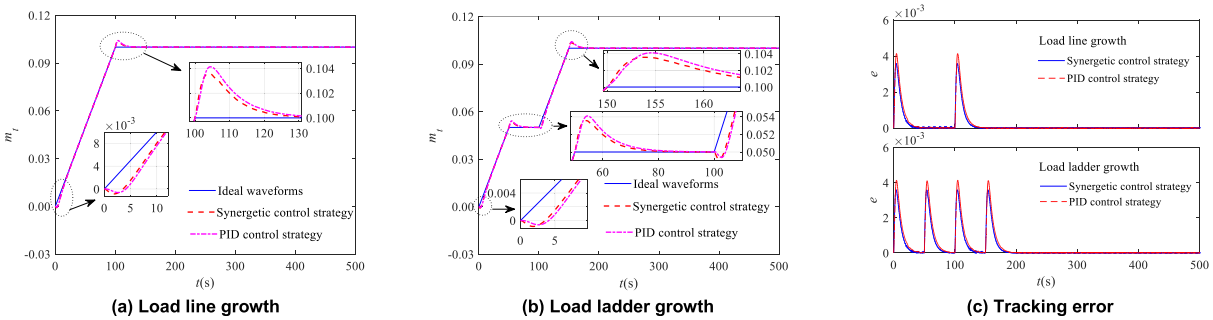


**FIGURE 8.** Ideal waveforms tracking process of load growth.

## V. ROBUSTNESS AND APPLICABILITY OF SYNERGETIC CONTROL STRATEGY

In this section, the robustness of the synergetic control strategy is analyzed. First, the basic method of robustness analysis is given. Then, the robustness indexes of synergetic and PID control strategies are calculated and evaluated. Finally, the applicability of the synergetic control strategy is proved by analyzing the dynamic response of hydropower station under different parameters.

### A. BASIC METHOD OF ROBUSTNESS

Robustness is an important index to evaluate the performance of controller. It refers to the characteristics of the system to maintain the original performance under the disturbance of parameter [48]. In this study, the index of quantitative analysis is applied to evaluate the robustness of the control strategy.

Specifically, for a system of the following form:

$$\boldsymbol{R} = \boldsymbol{R}(\boldsymbol{S}, \boldsymbol{T}) \tag{30}$$

where, $\boldsymbol{S} = (S_1, S_2, \ldots, S_l)^{\mathrm{T}}$ is the $l$-dimensional vector of the design variables, and $\boldsymbol{T} = (T_1, T_2, \ldots, T_m)^{\mathrm{T}}$ is the $m$-dimensional vector of the design parameters, $\boldsymbol{R} = (R_1, R_2, \ldots, R_n)^{\mathrm{T}}$ is a performance function represented by an $m$-dimensional vector.

The Jacobian matrix representing system sensitivity is shown below:

$$\boldsymbol{J} = [\boldsymbol{J_S}, \boldsymbol{J_T}] = \left[\frac{\partial \boldsymbol{R}}{\partial \boldsymbol{S}}, \frac{\partial \boldsymbol{R}}{\partial \boldsymbol{T}}\right] \tag{31}$$

A system is considered to be robust when its sensitivity to change is low. Ideally, all singular values of the sensitivity Jacobian matrix can be minimized. Accordingly, the Vandermond norm of Jacobian matrix is used as the measure index of robustness, and the following equation is given [49].

$$RI = \|\boldsymbol{J}\|_{Frob} \tag{32}$$

where, RI is index of robustness, $\|.\|_{Frob}$ is *Frobenius* norm.

### B. ANALYSIS OF ROBUSTNESS

According to the robustness analysis method, for HSDC, the design variables $\boldsymbol{S} = (y, q_t, x_t)^{\mathrm{T}}$, designed parameters $\boldsymbol{T} = (K, T_{wt}, m_g)^{\mathrm{T}}$, and $\boldsymbol{R} = (\dot{y}, \dot{q}_t, \dot{x}_t)^{\mathrm{T}}$ is taken. The RI is calculated based on synergetic and PID control strategy under different values of $K$, $T_{wt}$, $m_g$, which is given in Table 4.

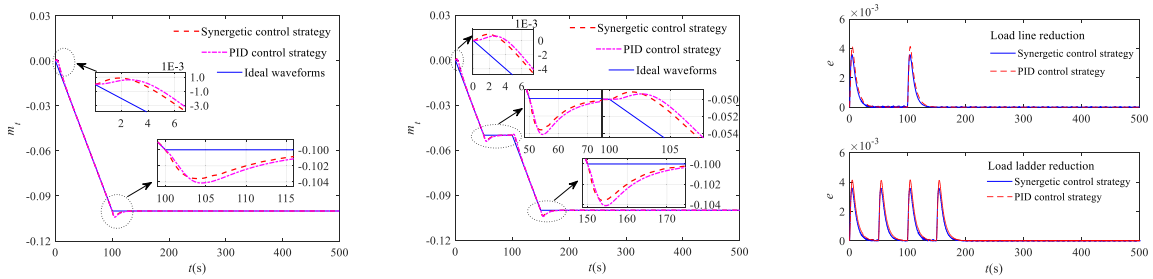


(a) Load line reduction (b) Load ladder reduction (c) Tracking error

**FIGURE 9.** Ideal waveforms tracking process of load reduction.

**TABLE 4.** Ri of HSDC under synergetic control strategy, PID control strategy and various parameters.

| Designed Parameters | Values | RI | |
|---|---|---|---|
| | | Synergetic Control strategy | PID Control strategy |
| $K$ (s/m$^2$) | 0.004 | 1.65832 | 3.05787 |
| | 0.024 | 1.66395 | 3.05787 |
| | 0.044 | 1.66961 | 3.05787 |
| | 0.064 | 1.67530 | 3.05787 |
| $T_{wt}$ (s) | 2.83 | 1.65832 | 3.05787 |
| | 3.83 | 1.73611 | 3.05787 |
| | 4.83 | 1.78519 | 3.05787 |
| | 5.83 | 1.81899 | 3.05787 |
| $m_g$ (s) | -0.10 | 1.65832 | 3.05787 |
| | -0.05 | 1.65985 | 3.05787 |
| | 0.05 | 1.67358 | 3.05787 |
| | 0.10 | 1.68569 | 3.05787 |
| $e_x$ | -1.1 | 0.18548 | 1.19386 |
| | -1.0 | 0.18583 | 1.19339 |
| | -0.9 | 0.18618 | 1.19293 |
| | -0.8 | 0.18653 | 1.19246 |
| $e_y$ | 0.9 | 0.22525 | 1.19339 |
| | 1.0 | 0.18583 | 1.19339 |
| | 1.1 | 0.15790 | 1.19340 |
| | 1.2 | 0.13784 | 1.19340 |
| $e_h$ | 1.4 | 0.18442 | 1.12191 |
| | 1.5 | 0.18583 | 1.19339 |
| | 1.6 | 0.18712 | 1.26534 |
| | 1.7 | 0.18832 | 1.33769 |
| $e_{qx}$ | -0.1 | 0.18677 | 1.19200 |
| | 0.0 | 0.18583 | 1.19339 |
| | 0.1 | 0.18491 | 1.19480 |
| | 0.2 | 0.18400 | 1.19620 |
| $e_{qy}$ | 0.9 | 0.18437 | 1.08732 |
| | 1.0 | 0.18583 | 1.19339 |
| | 1.1 | 0.18825 | 1.30211 |
| | 1.2 | 0.19165 | 1.41285 |
| $e_{qh}$ | 0.3 | 0.20386 | 3.02523 |
| | 0.4 | 0.19115 | 1.77421 |
| | 0.5 | 0.18583 | 1.19339 |
| | 0.6 | 0.18312 | 0.87676 |

Table 4 indicates the following results:

(1) For different $K$, $T_{wt}$, $m_g$, the RI of HSDC is about 1.67 under synergetic control strategy while it is about 3.06 under the latter. According to the different six parameters of turbines, the value of RI is about 0.18 under synergetic control strategy and about 1.20 under PID control strategy. Obviously, the RI of HSDC under the former is smaller, which indicates that HSDC under the synergetic control strategy has stronger anti-interference ability, that is, strong robustness.

(2) Under the synergetic control strategy, the RI value of HSDC is positively correlated with each parameter., the RI becomes larger as the $K, T_{wt}, m_g$ increases. Moreover, the RI of HSDC under the increasing load is larger than that of decreasing load. Specifically, the more obvious the relationship between downstream water level and flow is, the larger the flow inertia time constant in penstock is and the larger the load disturbance is, the larger RI is. However, the RI of HSDC hardly changes with each parameter under PID control strategy. The value of RI is getting bigger as $e_x$, $e_h$, and $e_{qy}$ increase, while it decreases with the increase of the $e_y, e_{qx}, e_{qh}$ under synergetic control strategy. However, for HSDC under PID control strategy, the RI shows an increasing trend with the increase of $e_y$, $e_h$, $e_{qx}$ and $e_{qy}$, but it's the opposite of $e_x$ and $e_{qh}$.

Above all, it shows that the synergetic control strategy makes the anti-interference of the HSDC stronger, no matter for the change of the layout form of the HSDC or the variation of the operating condition point of turbine.

For HSDCST, the design variables $\boldsymbol{S} = (y, q_y, z, q_t, x_t)^{\mathrm{T}}$, and the designed parameters is selected as $\boldsymbol{T} = (K, T_{wy}, F, T_{wt}, m_g)^{\mathrm{T}}$, and $R = \left(\dot{y}, \dot{q}_y, \dot{z}, \dot{q}_t, \dot{x}_t\right)^{\mathrm{T}}$ is taken. It is given in Table 5 that the RI under synergetic, PID control strategy, and various parameters.

Table 5 indicates the following results:

(1) Under different values of $K, T_{wy}, F, T_{wt}, m_g$, there is an obvious difference in the RI of HSDCST under different control strategy. Specially, the RI is significantly smaller under synergetic control strategy in comparison with PID control strategy. The former is around 2.2 while the latter is around 3.3. The value of RI is around 0.25 for the variation of six parameters under synergetic control strategy and about 1.30 under PID control strategy. This indicates that HSDCST will have strong robustness when adopting the synergetic control strategy.

(2) For HSDCST under synergetic control strategy, the more obvious the downstream water level changes, and the greater the value of RI is. A change of the flow inertia time constant in tailwater tunnel cannot causes a variation of RI while it increases with the increase of the flow time constant of penstock. The RI hardly changes as the sectional area of surge tank increases. Load increment or load decrement will change the value of RI, which has a weak positive correlation with the amount of load variation. As far as the six parameters of HSDCST are concerned, their variation relationship with RI is the same as that of HSDC, whether under synergetic control strategy or PID control strategy. This indicates that

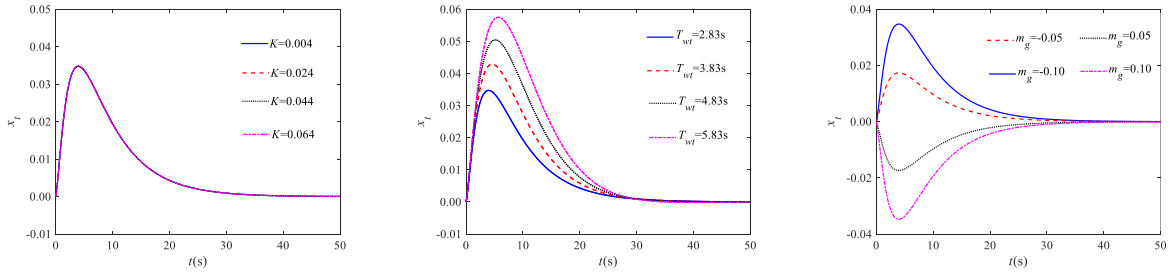


(a) $K$ (b) $T_{wt}$ (c) $m_g$

**FIGURE 10.** Dynamic response of $x_t$ in HSDC under synergetic control strategy and different values of $K$, $T_{wt}$, $m_g$.

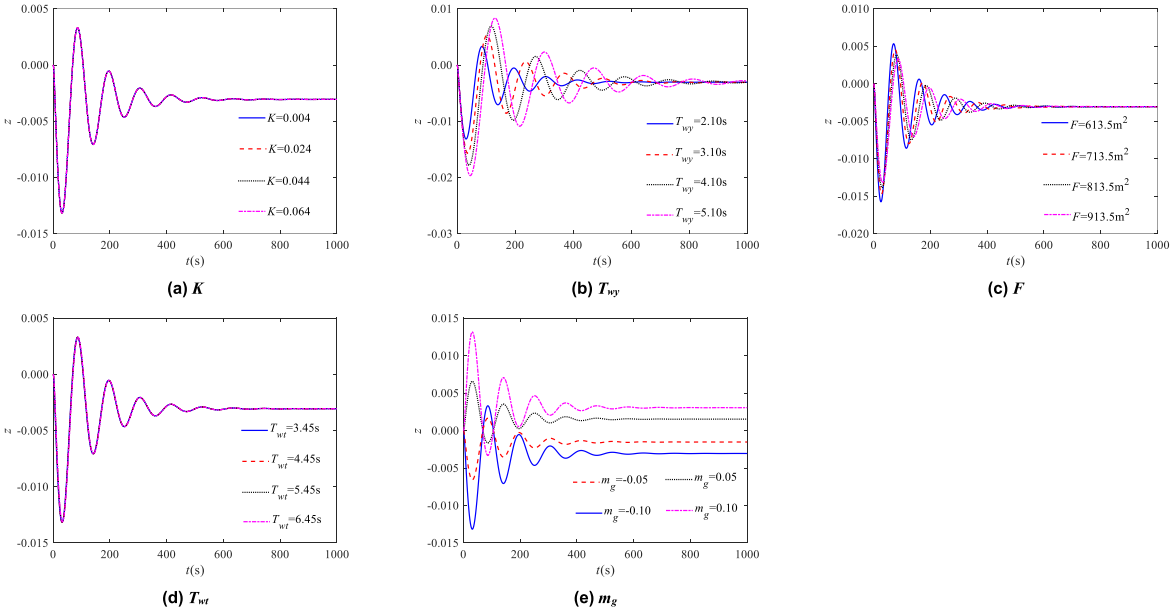


(a) $K$ (b) $T_{wy}$ (c) $F$

(d) $T_{wt}$ (e) $m_g$

**FIGURE 11.** Dynamic response of $z$ in HSDCST under synergetic control strategy and different values of $K$, $T_{wy}$, $F$, $T_{wt}$, $m_g$.

the synergetic control strategy responding to the variation of parameters in HSDCST has good robustness.

### C. ANALYSIS OF APPLICABILITY

Based on the engineering example of hydropower station in Section IV.A, the sensitivity analysis of $K$, $T_{wy}$, $T_{wt}$, $F$, and $m_g$ are carried out to prove that the applicability of synergetic control strategy for the water hammer wave in HSDC and mass wave in HSDCST. It is calculated according to (11) and (12) that the dynamic response of $x_t$ in HSDC and the dynamic response of $z$ in HSDCST under synergetic control strategy and different $K$, $T_{wy}$, $T_{wt}$, $F$, $m_g$, which are shown in Fig. 10 and Fig. 11.

As is shown in Fig. 10, it reflects the applicability of synergetic control strategy for water hammer wave in HSDC. The change of $K$ has little effect on the dynamic response of $x_t$ under the synergetic control strategy. The amplitude of dynamic response of $x_t$ increases obviously with the increase of $T_{wt}$, and the settling time becomes greater. The sign and variation of $m_g$ have obvious influence on the dynamic response of $x_t$. Specifically, the sign of $x_t$ is always opposite to $m_g$, and the amplitude and settling time of $x_t$ will increase as the $m_g$ increases. However, their equilibrium point of $x_t$ does not change under synergetic control strategy with $T_{wt}$, $m_g$ and $K$.

From Fig. 11, it can get the applicability of synergetic control strategy for mass wave in HSDCST. The dynamic response of $z$ has no obvious change under various $K$ and $T_{wt}$. However, $T_{wy}$, $F$, $m_g$ have an apparent effect on the dynamic response of $z$. Thereinto, the expansion of $F$ is beneficial to the dynamic quality of $z$, which will lead to a shorter amplitude and settling time of the dynamic response of $z$. The amplitude and settling time of the dynamic response of $z$ will become larger, which means that the dynamic response quality will become worse with the increase of $T_{wy}$. The equilibrium point remains the same under the different $K$, $T_{wt}$, $T_{wy}$, and $F$. The influence of $m_g$ on $z$ in HSDCST is the same as that on $x_t$ in HSDC, but the equilibrium point of $z$ is larger as the value of $m_g$ increases.

The above shows that the synergetic control strategy has excellent applicability for both water hammer wave of HSDC and mass wave of HSDCST.

## VI. SUMMARY AND CONCLUSION

For HSDC and HSDCST, the nonlinear mathematical model considering the relationship between downstream water level

**TABLE 5. Ri of HSDCST under synergetic control strategy, PID control strategy and various parameters.**

| Designed Parameters | Values | RI | |
|---|---|---|---|
| | | Synergetic Control strategy | PID Control strategy |
| $K$ (s/m$^2$) | 0.004 | 2.20883 | 3.32254 |
| | 0.024 | 2.21904 | 3.32254 |
| | 0.044 | 2.22933 | 3.32254 |
| | 0.064 | 2.23969 | 3.32254 |
| $T_{wy}$ (s) | 2.10 | 2.20883 | 3.32254 |
| | 3.10 | 2.20882 | 3.32253 |
| | 4.10 | 2.20882 | 3.32253 |
| | 5.10 | 2.20882 | 3.32253 |
| $F$ (m$^2$) | 913.5 | 2.20883 | 3.32254 |
| | 813.5 | 2.20884 | 3.32254 |
| | 713.5 | 2.20884 | 3.32254 |
| | 613.5 | 2.20885 | 3.32254 |
| $T_{wt}$ (s) | 3.45 | 2.20883 | 3.32254 |
| | 4.45 | 2.21148 | 3.32254 |
| | 5.45 | 2.21264 | 3.32254 |
| | 6.45 | 2.21324 | 3.32254 |
| $m_g$ | -0.10 | 2.20883 | 3.32254 |
| | -0.05 | 2.20836 | 3.32254 |
| | 0.05 | 2.20826 | 3.32254 |
| | 0.10 | 2.20859 | 3.32254 |
| $e_x$ | -1.1 | 0.25611 | 1.30658 |
| | -1.0 | 0.25612 | 1.30596 |
| | -0.9 | 0.25614 | 1.30534 |
| | -0.8 | 0.25615 | 1.30473 |
| $e_y$ | 0.9 | 0.31856 | 1.30596 |
| | 1.0 | 0.25612 | 1.30596 |
| | 1.1 | 0.21220 | 1.30596 |
| | 1.2 | 0.18042 | 1.30596 |
| $e_h$ | 1.4 | 0.25246 | 1.22767 |
| | 1.5 | 0.25612 | 1.30596 |
| | 1.6 | 0.25989 | 1.38476 |
| | 1.7 | 0.26375 | 1.46399 |
| $e_{qx}$ | -0.1 | 0.25622 | 1.30412 |
| | 0.0 | 0.25612 | 1.30596 |
| | 0.1 | 0.25603 | 1.30781 |
| | 0.2 | 0.25592 | 1.30967 |
| $e_{qy}$ | 0.9 | 0.25142 | 1.19077 |
| | 1.0 | 0.25613 | 1.30596 |
| | 1.1 | 0.26185 | 1.42405 |
| | 1.2 | 0.26856 | 1.54438 |
| $e_{qh}$ | 0.3 | 0.27344 | 3.30811 |
| | 0.4 | 0.26182 | 1.93938 |
| | 0.5 | 0.25613 | 1.30596 |
| | 0.6 | 0.25287 | 0.96137 |

and flow are established. The controller equation of HSDC and HSDCST are derived based on the synergetic control theory. Furthermore, the dynamic characteristics of HSDC and HSDCST under synergetic and PID control strategy are analyzed. Moreover, the robustness and applicability of synergetic control strategy for HDSC and HSDCST are studied. The following conclusions can be drawn from this investigation.

(1) The design of synergetic control strategy for HSDC and HSDCST contains two steps. The first step is the exact linearization for the state equation of HSDC and HSDCST. The second step is to select the appropriate macro variables to ensure that it can quickly converge to manifold. Finally, the control formula is obtained by solve the attenuation equation.

(2) The synergetic control strategy is superior to the PID control strategy under various disturbances in controlling the amplitude of water hammer wave in HSDC, which is down 12.5%. The attenuation of mass wave in HSDCST under synergetic control strategy is faster, and the settling time is 6.16s less than that of PID control strategy. It is under synergetic control strategy in comparison with PID control strategy that the dynamic characteristics of HSDC and HSDCST have rapid response, small overshoot, fast convergence speed and no static error for various disturbances.

(3) The value of RI is susceptible to the changes of $K$, $T_{wt}$, $m_g$, $e_x$, $e_h$, $e_y$, $e_{qx}$, $e_{qh}$, $e_{qy}$ and insensitive to the variation of $F$, $T_{wy}$. Specifically, RI value is about 1.65, 0.18 for HSDC and 2.21, 0.25 for HSDCST under synergetic control strategy, while it is about 3.05, 1.20 and 3.32, 1.30 under PID control strategy. It is much smaller under synergetic control strategy than PID control strategy. That is, the robustness of synergetic control strategy is more excellent than that of PID control strategy for HSDC and HSDCST.

(4) For the control effectiveness of ideal wave, the synergistic strategy has a better control effect whether in local load variation or overall tracking. Under synergetic control strategy, the dynamic response of load has faster response speed, smaller overshoot, and smaller process errors. The quantitative indicators of tracking effectiveness under synergetic control strategy is more excellent, which is reflected in smaller error, $\sigma$ and ISTSE than that under the PID control strategy.

(5) The dynamic performance of $x_t$ and $z$ are maintained at a high level under different parameters and synergetic control strategy. which has an excellent applicability. It proves that the synergetic control strategy has preeminent applicability in the control of water hammer wave in HSDC and mass wave in HSDCST.

In the future, the following work will be fully addressed.

(1) It is limited by various constraints in actual hydropower station operation, such as the dead zone of state variables, saturation limit of output variables will lead to the system trajectory cannot converge to manifold, reducing the control performance. It is worth further studying that integrating constraints into the design of controller.

(2) From the theoretical derivation and simulation results, the control method has high superiority. However, it is necessary to test its dynamic performance, anti-jamming capability, and the degree of matching with the hydropower unit, on the basis of which its control parameters is adjusted through the application of hydropower station.

(3) ADRC controller has good control performance, which is via internal state and uncertain factors of the system for real-time estimation and compensation, and ADRC has obtained the immunity function and is not dependent on the accurate mathematical model of the controlled. It has been used successfully in many fields and get excellent performance. The effect of ADRC on hydropower units is very promising.

## APPENDIX A

### A. THE EXPANSION EXPRESSION OF EQUILIBRIUM POINT IN (17) IS GIVEN AS FOLLOWS

$$\begin{cases} y_{E1} = \dfrac{e_{qh}m_g - e_h\left[\dfrac{\sqrt{\left[\frac{8h_{t0}}{H_0}+\frac{4}{e_{qh}}+\frac{4e_he_{qy}}{e_{qh}^2e_y-e_{qh}e_{qy}e_h}\right]\left[\frac{2h_{t0}}{H_0}+\frac{1}{e_{qh}}+\frac{K\sqrt{Q_0}}{H_0}+\frac{e_{qy}\left(m_ge_{qh}+e_h\right)}{e_{qh}^2e_y-e_{qh}e_{qy}e_h}\right]+\frac{K^2Q_0}{H_0^2}}+\frac{K\sqrt{Q_0}}{H_0}}{4\left[\frac{2h_{t0}}{H_0}+\frac{1}{e_{qh}}+\frac{e_he_{qy}}{e_{qh}^2e_y-e_{qh}e_{qy}e_h}\right]^2}-1\right]}{e_ye_{qh}-e_he_{qy}} \\ q_{tE1} = \dfrac{\sqrt{\left[\frac{8h_{t0}}{H_0}+\frac{4}{e_{qh}}+\frac{4e_he_{qy}}{e_{qh}^2e_y-e_{qh}e_{qy}e_h}\right]\left[\frac{2h_{t0}}{H_0}+\frac{1}{e_{qh}}+\frac{K\sqrt{Q_0}}{H_0}+\frac{e_{qy}\left(m_ge_{qh}+e_h\right)}{e_{qh}^2e_y-e_{qh}e_{qy}e_h}\right]+\frac{K^2Q_0}{H_0^2}}+\frac{K\sqrt{Q_0}}{H_0}}{4\left[\frac{2h_{t0}}{H_0}+\frac{1}{e_{qh}}+\frac{e_he_{qy}}{e_{qh}^2e_y-e_{qh}e_{qy}e_h}\right]^2}-1 \\ x_{tE1}=0 \end{cases}$$

### B. THE EXPANSION EXPRESSION OF EQUILIBRIUM POINT IN (18) IS GIVEN AS FOLLOWS

$$\begin{cases} q_{tE2} = \dfrac{m_ge_{qh}}{\left(e_{qh}e_y-e_he_{qy}\right)\left(\frac{2h_{t0}+2h_{y0}}{H_0}+\frac{1}{e_{qh}}+\frac{e_he_{qy}}{e_{qh}^2e_y-e_he_{qh}e_{qy}}\right)}+\dfrac{\frac{2h_{t0}+2h_{y0}}{H_0}+\frac{1}{e_{qh}}+\frac{K\sqrt{Q_0}}{H_0}+\frac{e_he_{qy}}{e_{qh}^2e_y-e_he_{qh}e_{qy}}-1}{\frac{2h_{t0}+2h_{y0}}{H_0}+\frac{1}{e_{qh}}+\frac{e_he_{qy}}{e_{qh}^2e_y-e_he_{qh}e_{qy}}} \\ \quad+\dfrac{\frac{K\sqrt{Q_0}}{H_0}\left[\frac{2h_{t0}+2h_{y0}}{H_0}+\frac{1}{e_{qh}}+\frac{e_he_{qy}}{e_{qh}^2e_y-e_he_{qh}e_{qy}}\left(\frac{2h_{t0}+2h_{y0}}{H_0}+\frac{1}{e_{qh}}+\frac{K\sqrt{Q_0}}{H_0}+\frac{e_he_{qy}+e_{qh}e_{qy}m_g}{e_{qh}^2e_y-e_he_{qh}e_{qy}}+\frac{KQ_0^2}{H_0^2}\right)\right]^{\frac{1}{2}}}{\left(\frac{2h_{t0}+2h_{y0}}{H_0}+\frac{1}{e_{qh}}+\frac{e_he_{qy}}{e_{qh}^2e_y-e_he_{qh}e_{qy}}\right)^2} \\ q_{yE2}=q_{tE2} \\ y_{E2} = -\dfrac{e_h}{e_{qh}e_y-e_he_{qy}}q_{tE2}+\dfrac{e_{qh}}{e_{qh}e_y-e_he_{qy}}m_g \\ x_{tE2}=0 \\ z_{E2} = -\left(\dfrac{2h_{t0}}{H_0}+\dfrac{1}{e_{qh}}+\dfrac{e_he_{qy}}{e_{qh}^2e_y-e_he_{qh}e_{qy}}\right)q_{tE2}++\dfrac{e_{qh}}{e_{qh}e_y-e_he_{qy}}m_g \end{cases}$$

### C. THE EXPRESSION OF $\eta_I$, $\xi_I$, $F_1[X]$ AND $G_1[X]$ IN (19) ARE SHOWN AS FOLLOWS

$$\eta_1 = \frac{1}{T_a}\frac{e_ye_{qh}-e_he_{qy}}{e_{qh}},\quad \eta_2 = \frac{1}{T_a}\frac{e_h}{e_{qh}},\quad \eta_3 = \frac{1}{T_a}\left(e_x-e_g-\frac{e_he_{qx}}{e_{qh}}\right)$$

$$\xi_1 = \frac{1}{T_a}\left(-\frac{1}{T_y}+\frac{1}{T_a}\frac{e_xe_{qh}-e_ge_{qh}-e_he_{qx}}{e_{qh}}\right)\left(e_y-\frac{e_he_{qy}}{e_{qh}}\right)+\frac{1}{T_{wt}T_a}\frac{e_he_{qy}}{e_{qh}^2},$$

$$\xi_2 = -\frac{1}{T_aT_{wt}}\frac{e_h}{e_{qh}}\left(\frac{2h_{t0}}{H_0}+\frac{1}{e_{qh}}\right)+\frac{1}{T_a}\left(e_x-e_g-\frac{e_he_{qx}}{e_{qh}}\right),\quad \xi_3 = \frac{1}{T_{wt}}\frac{K\sqrt{Q_0}}{H_0},\quad \xi_4 = \frac{1}{T_aT_{wt}}\frac{e_he_{qx}}{e_{qh}^2}+1$$

$$f_1(X) = \begin{bmatrix} \frac{1}{T_y}y \\ \frac{1}{T_{wt}}\left[\frac{K\sqrt{Q_0}}{H_0}\left(1-\sqrt{q_t+1}\right)-\left(\frac{2h_{t0}}{H_0}+\frac{1}{e_{qh}}\right)q_t+\frac{e_{qx}}{e_{qh}}x_t+\frac{e_{qy}}{e_{qh}}y\right] \\ \frac{1}{T_a}\left[\frac{e_h}{e_{qh}}q_t+\left(e_x-e_g-\frac{e_he_{qx}}{e_{qh}}\right)x_t+\left(e_y-\frac{e_he_{qy}}{e_{qh}}\right)y-m_g\right] \end{bmatrix},$$

$$g_1(X) = \left[\frac{1}{T_y},0,0\right]^{\mathrm{T}}$$

### D. THE EXPRESSION OF $A_I$, $B_I$, $C_I$, $D_I$, $F_2[X]$ AND $G_2[X]$ IN (20) ARE GIVEN AS FOLLOWS

$$
\begin{aligned}
a_1 &= \frac{1}{T_a}\frac{e_y e_{qh} - e_h e_{qy}}{e_{qh}}, \quad a_2 = \frac{1}{T_a}\frac{e_h}{e_{qh}}, \quad a_3 = \frac{1}{T_a}\left(e_x - e_g - \frac{e_h e_{qx}}{e_{qh}}\right)\\
b_1 &= \frac{1}{T_a}\left(-\frac{1}{T_y} + \frac{1}{T_a}\frac{e_x e_{qh} - e_g e_{qh} - e_h e_{qx}}{e_{qh}}\right)\left(e_y - \frac{e_h e_{qy}}{e_{qh}}\right) + \frac{1}{T_{wt}T_a}\frac{e_h e_{qy}}{e_{qh}^2},\\
b_2 &= -\frac{1}{T_a T_{wt}}\frac{e_h}{e_{qh}}\left(\frac{2h_{t0}}{H_0} + \frac{1}{e_{qh}}\right) + \frac{1}{T_a}\left(e_x - e_g - \frac{e_h e_{qx}}{e_{qh}}\right), \quad b_3 = -\frac{1}{T_a T_{wt}}\frac{e_h}{e_{qh}}, \quad b_4 = \frac{1}{T_a T_{wt}}\frac{e_h e_{qx}}{e_{qh}^2} + 1,\\
c_1 &= -\frac{b_1}{T_y} + \frac{b_2}{T_{wt}}\frac{e_{qy}}{e_{qh}} + \frac{b_4}{T_a}\left(e_x - e_g - \frac{e_h e_{qx}}{e_{qh}}\right), \quad c_2 = -\frac{b_2}{T_{wt}}\left(\frac{1}{e_{qh}} + \frac{2h_{t0}}{H_0}\right) + \frac{b_3 Q_0}{FH_0} + \frac{b_4}{T_a}\frac{e_h}{e_{qh}},\\
c_3 &= -\frac{b_2}{T_{wt}}, \quad c_4 = \frac{-b_3 Q_0}{FH_0},\\
c_5 &= \frac{b_2}{T_{wt}}\frac{e_{qx}}{e_{qh}} + \frac{b_4}{T_a}\left(e_x - e_g - \frac{e_h e_{qx}}{e_{qh}}\right), \quad d_1 = -\frac{c_1}{T_y} + \frac{c_2}{T_{wt}}\frac{e_{qy}}{e_{qh}} + \frac{d_5}{T_a}\left(e_x - e_g - \frac{e_h e_{qx}}{e_{qh}}\right),\\
d_3 &= -\frac{c_2}{T_{wt}} + \frac{c_4}{T_{wy}}, \quad d_5 = \frac{c_4 K\sqrt{Q_0}}{2H_0}\\
d_2 &= -\frac{c_2}{T_{wt}}\left(\frac{1}{e_{qh}} + \frac{2h_{t0}}{H_0}\right) + \frac{c_3 Q_0}{FH_0} + \frac{c_5}{T_a}\frac{e_h}{e_{qh}}, \quad d_4 = -\frac{c_3 Q_0}{FH_0} - \frac{2c_4 h_{y0}}{H_0},\\
d_6 &= \frac{c_2}{T_{wt}}\frac{e_{qx}}{e_{qh}} + \frac{c_5}{T_a}\left(e_x - e_g - \frac{e_h e_{qx}}{e_{qh}}\right)
\end{aligned}
$$

$$
f_2(X) = \begin{bmatrix}
-\frac{1}{T_y}y \\
\frac{1}{T_{wt}}\left[-z - \left(\frac{1}{eqh} + \frac{2h_{t0}}{H_0}\right)q_t - \frac{e_{qx}}{e_{qh}}x_t - \frac{e_{qy}}{e_{qh}}y\right] \\
\frac{1}{T_F}\left(q_t - q_y\right) \\
\frac{1}{T_{wy}}\left[z - \frac{K\sqrt{Q_0}}{H_0}\left(\sqrt{q_y + 1} - 1\right) - \frac{2h_{y0}}{H_0}\right] \\
\frac{1}{T_a}\left[\frac{e_h}{e_{qh}}q_t + \left(e_x - e_g - \frac{e_h e_{qx}}{e_{qh}}\right)x_t + \left(e_y - \frac{e_h e_{qy}}{e_{qh}}\right)y - m_g\right]
\end{bmatrix},
$$

$$
g_2(X) = \left[\frac{1}{T_y}, 0, 0, 0, 0, 0\right]^T
$$

### E. THE EXPRESSION OF HSDC UNDER PID CONTROL STRATEGY ARE PRESENTED AS FOLLOWS

$$
\begin{cases}
\dot{y} = \dfrac{1}{T_y}(u - y)\\
\dot{q}_t = \dfrac{1}{T_{wt}}\left[\dfrac{K\sqrt{Q_0}}{H_0}\left(1 - \sqrt{q_t + 1}\right) - \left(\dfrac{2h_{t0}}{H_0} + \dfrac{1}{e_{qh}}\right)q_t + \dfrac{e_{qx}}{e_{qh}}x_t + \dfrac{e_{qy}}{e_{qh}}y\right]\\
\dot{x}_t = \dfrac{1}{T_a}\left[\dfrac{e_h}{e_{qh}}q_t + \left(e_x - e_g - \dfrac{e_h e_{qx}}{e_{qh}}\right)x_t + \left(e_y - \dfrac{e_h e_{qy}}{e_{qh}}\right)y - m_g\right]\\
\dot{u} = -\dfrac{K_p}{T_a}\left[\dfrac{e_h}{e_{qh}}q_t + \left(e_x - e_g - \dfrac{e_h e_{qx}}{e_{qh}}\right)x_t + \left(e_y - \dfrac{e_h e_{qy}}{e_{qh}}\right)y - m_g\right] - K_i x_t\\
- \dfrac{K_d}{T_a}\left\{\dfrac{e_h}{e_{qh}}\dfrac{1}{T_{wt}}\left[\dfrac{K\sqrt{Q_0}}{H_0}\left(1 - \sqrt{q_t + 1}\right) - \left(\dfrac{2h_{t0}}{H_0} + \dfrac{1}{e_{qh}}\right)q_t + \dfrac{e_{qx}}{e_{qh}}x_t + \dfrac{e_{qy}}{e_{qh}}y\right]\right.\\
\left. + \dfrac{e_x e_{qh} - e_g e_{qh} - e_h e_{qx}}{T_a e_{qh}}\left[\dfrac{e_h}{e_{qh}}q_t + \left(e_x - e_g - \dfrac{e_h e_{qx}}{e_{qh}}\right)x_t + \left(e_y - \dfrac{e_h e_{qy}}{e_{qh}}\right)y - m_g\right] + \dfrac{e_y e_{qh} - e_h e_{qy}}{T_y e_{qh}}(u - y)\right\}
\end{cases}
$$

### F. THE EXPRESSION OF HSDCST UNDER PID CONTROL STRATEGY ARE PRESENTED AS FOLLOWS

$$
\begin{cases}
\dot{y} = \dfrac{1}{T_y}(u - y) \\
\dot{q}_t = \dfrac{1}{T_{wt}}\left[-z - \left(\dfrac{1}{eqh} + \dfrac{2h_{t0}}{H_0}\right) q_t - \dfrac{e_{qx}}{e_{qh}} x_t - \dfrac{e_{qy}}{e_{qh}} y\right] \\
\dot{z} = \dfrac{1}{T_F}(q_t - q_y) \\
\dot{q}_y = \dfrac{1}{T_{wy}}\left[z - \dfrac{K\sqrt{Q_0}}{H_0}\left(\sqrt{q_y + 1} - 1\right) - \dfrac{2h_{y0}}{H_0}\right] \\
\dot{x}_t = \dfrac{1}{T_a}\left[\dfrac{e_h}{e_{qh}} q_t + \left(e_x - e_g - \dfrac{e_h e_{qx}}{e_{qh}}\right) x_t + \left(e_y - \dfrac{e_h e_{qy}}{e_{qh}}\right) y - m_g\right] \\
\dot{u} = -\dfrac{K_p}{T_a}\left[\dfrac{e_h}{e_{qh}} q_t + \left(e_x - e_g - \dfrac{e_h e_{qx}}{e_{qh}}\right) x_t + \left(e_y - \dfrac{e_h e_{qy}}{e_{qh}}\right) y - m_g\right] - K_i x_t \\
\quad -\dfrac{K_d}{T_a}\left\{\begin{array}{l}
\dfrac{e_h}{e_{qh} T_{wt}}\left[-z - \left(\dfrac{1}{eqh} + \dfrac{2h_{t0}}{H_0}\right) q_t - \dfrac{e_{qx}}{e_{qh}} x_t - \dfrac{e_{qy}}{e_{qh}} y\right] - \dfrac{e_y e_{qh} - e_h e_{qy}}{e_{qh} T_y}(u - y) \\
\quad + \dfrac{e_x e_{qh} - e_g e_{qh} - e_h e_{qx}}{e_{qh} T_a}\left[\dfrac{e_h}{e_{qh}} q_t + \left(e_x - e_g - \dfrac{e_h e_{qx}}{e_{qh}}\right) x_t + \left(e_y - \dfrac{e_h e_{qy}}{e_{qh}}\right) y - m_g\right]
\end{array}\right\}
\end{cases}
$$

## REFERENCES


[1] Q. Z. Liu and M. Hu, "Typical layout and construction of hydropower station," in *Hydropower Station*. Beijing, China: China Water Power Press, 2010, pp. 108–112.

[2] L. Yu, X. Wu, S. Wu, B. Jia, G. Han, P. Xu, J. Dai, Y. Zhang, F. Wang, Q. Yang, and Z. Zhou, "Multi-objective optimal operation of cascade hydropower plants considering ecological flow under different ecological conditions," *J. Hydrol.*, vol. 601, Oct. 2021, Art. no. 126599.

[3] Z. Zhang, H. Qin, L. Yao, Y. Liu, Z. Jiang, Z. Feng, S. Ouyang, S. Pei, and J. Zhou, "Downstream water level prediction of reservoir based on convolutional neural network and long short-term memory network," *J. Water Resour. Planning Manage.*, vol. 147, no. 9, pp. 1–15, Sep. 2021.

[4] H. Wang and J. D. Yang, "Effect of stage-discharge relation on guaranteed regulation of hydropower station transient," *J. Hydroelectr. Eng.*, vol. 34, pp. 153–160, Jan. 2015.

[5] D. Y. Zhu and W. C. Guo, "Setting condition of surge tank based on stability of hydro-turbine governing system considering nonlinear penstock head loss," *Int. J. Electr. Power Energy Syst.*, vol. 113, pp. 82–372, Dec. 2019.

[6] W. C. Guo, J. D. Yang, M. J. Wang, and X. Lai, "Nonlinear modeling and stability analysis of hydro-turbine governing system with sloping ceiling tailrace tunnel under load disturbance," *Energy Convers. Management.*, vol. 106, pp. 38–127, Dec. 2015.

[7] Z. Y. Peng and W. C. Guo, "Saturation characteristics for stability of hydro-turbine governing system with surge tank," *Renew. Energy.*, vol. 131, pp. 32–318, Feb. 2019.

[8] X. Xu and W. Guo, "Chaotic behavior of turbine regulating system for hydropower station under effect of nonlinear turbine characteristics," *Sustain. Energy Technol. Assessments*, vol. 44, Apr. 2021, Art. no. 101088.

[9] Z. Zhao, J. Yang, C. Y. Chung, W. Yang, X. He, and M. Chen, "Performance enhancement of pumped storage units for system frequency support based on a novel small signal model," *Energy*, vol. 234, Nov. 2021, Art. no. 121207.

[10] Z. Zhao, J. Yang, Y. Huang, W. Yang, W. Ma, L. Hou, and M. Chen, "Improvement of regulation quality for hydro-dominated power system: Quantifying oscillation characteristic and multi-objective optimization," *Renew. Energy*, vol. 168, pp. 606–631, May 2021.

[11] F. Qu and W. Guo, "Robust $H_\infty$ control for hydro-turbine governing system of hydropower plant with super long headrace tunnel," *Int. J. Electr. Power Energy Syst.*, vol. 124, Jan. 2021, Art. no. 106336.

[12] W. Guo and J. Yang, "Hopf bifurcation control of hydro-turbine governing system with sloping ceiling tailrace tunnel using nonlinear state feedback," *Chaos, Solitons Fractals*, vol. 104, pp. 426–434, Nov. 2017.

[13] S. Huang, B. Zhou, S. Bu, C. Li, C. Zhang, H. Wang, and T. Wang, "Robust fixed-time sliding mode control for fractional-order nonlinear hydro-turbine governing system," *Renew. Energy*, vol. 139, pp. 447–458, Aug. 2019.

[14] D. P. Wu, B. Yan, D. Liu, and Z. H. Xiao, "Study on improved sliding mode control strategy suitable for hydropower units," *J. Hydroelectr. Eng.*, vol. 10, pp. 82–91, Oct. 2020.

[15] W. Guo, "Nonlinear disturbance decoupling control for hydro-turbine governing system with sloping ceiling tailrace tunnel based on differential geometry theory," *Energies*, vol. 11, no. 12, p. 3340, Nov. 2018.

[16] J. B. Lu, X. R. Hou, and M. Luo, "Parametric stabilization method for a class of Hopf bifurcation systems," *J. Univ. Electron. Sci. Technol. China.*, vol. 45, pp. 944–949, Aug. 2016.

[17] Y.-Q. Ren, X.-G. Duan, H.-X. Li, and C. L. P. Chen, "Dynamic switching based fuzzy control strategy for a class of distributed parameter system," *J. Process Control*, vol. 24, no. 3, pp. 88–97, Mar. 2014.

[18] J. Zhao, L. Li, Z. Li, Z. Chen, L. Xiao, and G. Chen, "Multi-segment fuzzy control for start-up optimizing of LCC-based high-voltage power supply," *Energy Rep.*, vol. 8, pp. 552–559, Feb. 2022.

[19] J. Ren, Z. Chen, M. Sun, and Q. Sun, "Frequency performance analysis of proportional integral-type active disturbance rejection generalized predictive control for time delay systems," *Syst. Sci. Control Eng.*, vol. 10, no. 1, pp. 1–14, Dec. 2022.

[20] H. Wang, X. Wu, X. Zheng, and X. Yuan, "Virtual voltage vector based model predictive control for a nine-phase open-end winding PMSM with a common DC bus," *IEEE Trans. Ind. Electron.*, vol. 69, no. 6, pp. 5386–5397, Jun. 2022.

[21] J. Q. Han, "Auto disturbances rejection controller and its application," *Control Decis.*, vol. 13, pp. 19–23, Jan. 1998.

[22] P. Zhao, "Application of synergetic control theory in power system stability control," Huazhong Univ. Sci. Technol., Wuhan, China, Tech. Rep. TM76, Sep. 2013.

[23] Z. Jiang and R. A. Dougal, "Synergetic control of power converters for pulse current charging of advanced batteries from a fuel cell power source," *IEEE Trans. Power Electron.*, vol. 19, no. 4, pp. 1140–1150, Jul. 2004.

[24] E. Santi, A. Monti, D. Li, K. Proddutur, and R. A. Dougal, "Synergetic control for DC-DC boost converter: Implementation options," *IEEE Trans. Ind. Appl.*, vol. 39, no. 6, pp. 1803–1813, Nov. 2003.

[25] W. Zhu, Y. Zheng, J. Dai, and J. Zhou, "Design of integrated synergetic controller for the excitation and governing system of hydraulic generator unit," *Eng. Appl. Artif. Intell.*, vol. 58, pp. 79–87, Feb. 2017.

[26] J. Zhou, Y. Zhang, Y. Zheng, and Y. Xu, "Synergetic governing controller design for the hydraulic turbine governing system with complex conduit system," *J. Franklin Inst.*, vol. 355, no. 10, pp. 4131–4146, Jul. 2018.

[27] S. Huang, L. Xiong, J. Wang, P. Li, Z. Wang, and M. Ma, "Fixed-time synergetic controller for stabilization of hydraulic turbine regulating system," *Renew. Energy*, vol. 157, pp. 1233–1242, Sep. 2020.
[28] P. Zhao, J. Zhuo, Z. Li, W. Yao, and S. Wang, "Design of a nonlinear excitation controller using synergetic control theory," in *Proc. IEEE PES Asia–Pacific Power Energy Eng. Conf. (APPEEC)*, Dec. 2014, pp. 1–5.
[29] P. Zhao, Y. Wei, S. R. Wang, J. Y. Wen, and S. J. Cheng, "Decentralized nonlinear synergetic power system stabilizers design for power system stability enhancement," *Int. Trans. Electr. Energy Syst.*, vol. 33, pp. 115–122, Sep. 2013.
[30] J. Ni, C. Liu, K. Liu, and X. Pang, "Variable speed synergetic control for chaotic oscillation in power system," *Nonlinear Dyn.*, vol. 78, no. 1, pp. 681–690, Oct. 2014.
[31] Z. Bouchama, N. Essounbouli, M. N. Harmas, A. Hamzaoui, and K. Saoudi, "Reaching phase free adaptive fuzzy synergetic power system stabilizer," *Int. J. Electr. Power Energy Syst.*, vol. 77, pp. 43–49, May 2016.
[32] T. Ademoye and A. Feliachi, "Reinforcement learning tuned decentralized synergetic control of power systems," *Electr. Power Syst. Res.*, vol. 86, pp. 34–40, May 2012.
[33] G. E. Veselov, A. N. Popov, and I. A. Radionov, "Synergetic control of asynchronous electric traction drives of locomotives," *J. Comput. Syst. Sci. Int.*, vol. 53, no. 4, pp. 587–600, Jul. 2014.
[34] T. Zhang, J. Zhou, X. Lai, Y. Huang, and M. Li, "Nonlinear stability and dynamic characteristics of grid-connected hydropower station with surge tank of a long lateral pipe," *Int. J. Electr. Power Energy Syst.*, vol. 136, Mar. 2022, Art. no. 107654.
[35] T. Zhang, J. Zhou, X. Yang, and H. Li, "Multi-objective optimization and decision-making of the combined control law of guide vane and pressure regulating valve for hydroelectric unit," *Energy Sci. Eng.*, vol. 10, no. 2, pp. 472–487, Feb. 2021.
[36] X. Lai, C. Li, W. Guo, Y. Xu, and Y. Li, "Stability and dynamic characteristics of the nonlinear coupling system of hydropower station and power grid," *Commun. Nonlinear Sci. Numer. Simul.*, vol. 79, Dec. 2019, Art. no. 104919.
[37] W. Guo, J. Yang, M. Wang, and X. Lai, "Nonlinear modeling and stability analysis of hydro-turbine governing system with sloping ceiling tail-race tunnel under load disturbance," *Energy Convers. Manage.*, vol. 106, pp. 127–138, Dec. 2015.
[38] M. H. Chaudhry, "Surge tank," in *Applied Hydraulic Transients*. New York, NY, USA: 2014, pp. 314–342.
[39] *Limited HEC 2013 Research Report on the Operation Mode of Turbine Units of Jinping Hydropower Station II*, Huadong Eng. Corp. Ltd., Hangzhou, China, 2013.
[40] J. Lin, R. Xu, and L. Li, "Turing-hopf bifurcation of reaction-diffusion neural networks with leakage delay," *Commun. Nonlinear Sci. Numer. Simul.*, vol. 85, Jun. 2020, Art. no. 105241.
[41] S. P. Wei, "Dynamic characteristics of turbine regulating system," in *Hydraulic Turbine Regulation*, Wuhan, China: Huazhong Univ. Science Technology Press, 2009, pp. 77–132.
[42] T. Stein, "Frequency control under isolated network conditions," *Water Power.*, vol. 9, pp. 320–324, Sep. 1970.
[43] I. Pan and S. Das, "Frequency domain design of fractional order PID controller for AVR system using chaotic multi-objective optimization," *Int. J. Electr. Power Energy Syst.*, vol. 51, pp. 106–118, Oct. 2013.
[44] *Guide for Hydraulic Transient Guarantee Design of Hydropower Stations*, Standard NB/T 10342-2019, 2019.
[45] S. Q. Zhang, "Research on mechanism analysis and suppression technology with respect to EFT and surge," North China Electr. Power Univ., Baoding, China, Tech. Rep. TM86, Dec. 2003.
[46] S. Longo, V. Di Federico, and L. Chiapponi, "Non-newtonian power-law gravity currents propagating in confining boundaries," *Environ. Fluid Mech.*, vol. 15, no. 3, pp. 515–535, Jun. 2015.
[47] W. Guo, B. Wang, J. Yang, and Y. Xue, "Optimal control of water level oscillations in surge tank of hydropower station with long headrace tunnel under combined operating conditions," *Appl. Math. Model.*, vol. 47, pp. 260–275, Jul. 2017.
[48] J. Jiang, "Robust model-based fault diagnosis for dynamic systems," *Automatica*, vol. 38, no. 6, pp. 1089–1091, Jun. 2002.
[49] R. J. Patton, D. Putra, and S. Klinkhieo, "Friction compensation as a fault tolerant control problem," *Int. J. Syst. Sci.*, vol. 41, pp. 987–1001, Jul. 2010.

**TIANYU ZHANG** received the B.S. degree in energy and power engineering (hydrodynamic) from the North China University of Water Resources and Electric Power, in 2018. He is currently pursuing the Ph.D. degree in hydraulic engineering with the Huazhong University of Science and Technology. His research interests include the transition process and control of hydropower units.

**JIANZHONG ZHOU** is currently a Professor and the Doctoral Supervisor with the Huazhong University of Science and Technology, who is a major in the hydropower industry. His research interests include advanced theories and methods of hydropower energy and its complex system analysis, power generation process control-diagnosis-simulation, and high-performance network and information systems.

**YONGCHUAN ZHANG** is currently an Academician with the Chinese Academy of Engineering. He has deep attainments in the fields of water resources, electric power and energy, and has achieved a series of influential application achievements.

**YANG LIU** received the B.S. degree in hydropower engineering from China Three Gorges University, in 2019. He is currently pursuing the M.D. degree with the School of Civil and Hydropower Engineering, Huazhong University of Science and Technology. His research interests include the stability and dynamic characteristic of hydraulic transient process and the control strategies of hydro turbine governing systems.

**YUXIN LI** received the B.S. degree in hydropower engineering from the Kunming University of Science and Technology, in 2019, and she is currently pursuing the Ph.D. degree with the School of Civil and Hydraulic Engineering, Huazhong University of Science and Technology. Her research interest includes the calculation of hydraulic transient process of hydro turbines.